Use of the M&S Configuration in Theta Pinches *

G. H. WOLF

Institut für Plasmaphysik, Garching bei München

(Z. Naturforsch. **24 a**, 998—1021 [1969]; received 30 September 1968)

The M & S configuration ** gives equilibrium for a toroidal plasma without net current in the azimuthal direction and without rotational transform. Explicit solutions are obtained only for the restricted cases $\beta=0$, and $\beta \leqq 1$ in the surface current model, but configurations with continuous pressure profile are proved to exist. The use of the M & S configuration to confine a toroidal theta pinch plasma leads to problems in the establishment of the equilibrium and in particular in its stability.

The stability of the M & S configuration is investigated for the simplified case of the corrugated linear theta pinch, LIMPUS. This configuration is theoretically unstable with respect to $m \geqq 1$ flutes. Mechanisms to suppress these modes are based on finite gyroradii stabilisation for $m \geqq 2$, and on the conducting wall for $m=1$, the latter case being limited to very high β. No $m \geqq 2$ instabilities are observed experimentally, although $m=1$ instabilities with growth times agreeing with MHD theory are detected. An exrapolation of these results to an M & S configuration gives $\tau_{M\&S}/\tau_D \approx (\xi_0/r_p)^{1/2}$, where r_p is the average minor radius, ξ_0 an initial deviation from the M & S equilibrium position, and $\tau_{M\&S}$ and τ_D are the M & S confinement time and the toroidal drift time, respectively. M & S experiments with theta pinch plasmas near 10 eV, $\tau_{M\&S}$ is extended by a factor 3—4 beyond τ_D, which is in agreement with the above relation. This suggest firstly, that the M & S configurations investigated are an adequate approximation to the required equilibrium, and, secondly, that the MHD instabilities substantially limit the confinement time.

Simple models show that oscillating axial currents, a steady axial motion of the LIMPUS magnetic field configuration or a standing wave like oscillation can suppress the instabilities mentioned. Experiments on such dynamic stabilisation are in progress.

1. Introduction

The theta pinch has been useful in heating and confining a plasma [1, 2]. It may eventually be used in attempts to approach Lawson's criterion [3, 4] for thermonuclear energy production. In the theta pinches of interest here, a narrow cylindrical plasma column is compressed radially in a few μsec by means of a rapidly rising magnetic field parallel to the axis of the cylinder. The maximum magnetic field strength of above 10^5 Gauss [5, 6] is reached in about 10^{-5} sec. The shock heating and subsequent adiabatic compression of the plasma by this method increases the mean energy kT_i of the deuterons to 5 – 10 keV. This was determined from the yield of neutrons [7] due to fusion reactions, and from their energy spectrum [8]. The mean thermal energy of the electrons, kT_e, which can be determined for instance from the Doppler broadening of scattered laser light [9], or from soft X-ray emission, by comparison reaches values of only about 500 eV [8]. The particle density on the axis of the cylindrical plasma column, measured by interferometric methods [10] and from the emitted continuum radiation, reached about 2×10^{16} cm^{-3}.

Following the rapid compression of the plasma, after the radial oscillations have damped out, a stationary equilibrium is established between the plasma and the confining magnetic field. In the straight magentic field of an infinitely long coil,

* This work was performed as part of the research program of the Institut für Plasmaphysik, Garching, and Euratom.

** From F. MEYER and H. U. SCHMIDT and also from mud and snow tyre treads.

[1] W. C. ELMORE, E. M. LITTLE, and W. E. QUINN, Proc. II. Genv. Conf. **32**, P/356 [1958].

[2] A. C. KOLB, Phys. Rev. **112**, 291 [1958].

[3] J. D. LAWSON, Proc. Am. Phys. Soc. B **70**, 6 [1967].

[4] F. L. RIBE, T. A. OLIPHANT JR., and W. E. QUINN, Los Alamos Report LA-3294-MS [1965].

[5] W. E. QUINN, E. M. LITTLE, F. L. RIBE, W. B. RIESENFELD, and G. A. SAWYER, PPCNFR CN-21/92, Culham [1965].

[5a] „PPCNF . . .“ bedeutet: Plasma Physics and Controlled Nuclear Fusion Research, Conference Proceedings Culham 1965, Vienna 1966.

[6] C. ANDELFINGER, D. DECKER, E. FÜNFER, M. KEILHACKER, J. SOMMER, and M. ULRICH, PPCNFR, CN-21/49, Culham [1965].

[7] L. M. GOLDMAN, R. W. KILB, and H. C. POLLOCK, Phys. Fluids **7**, 1005 [1964].

[8] E. FÜNFER, Institut für Plasmaphysik, Report IPP 1/70 [1967] and Proc. Los Alamos Conf. [1967].

[9] E. FÜNFER, B. KRONAST, and H. J. KUNZE, Phys. Lett. **5**, 125 [1963].

[10] E. FÜNFER, K. HAIN, H. HEROLD, P. IGENBERGS, and F. P. KÜPPER, Z. Naturforsch. **17 a**, 967 [1962].

the radial drop of the plasma kinetic pressure p is compensated by an increase in the "magnetic pressure" $B^2/2\,\mu_0$ [11]. The local ratio of p to $p+B^2/2\,\mu_0$ is defined as β. $\beta=1$ thus refers to the extreme case of a plasma free from interior magnetic fields. In the theta pinches just described the maximum value of β occurs on the axis of the plasma cylinder following the fast compression. Its magnitude is not known exactly, e. g. due to an uncertainty in the ion temperature, it varies within the range of about $0.3<\beta<0.9$ [5, 6].

The confinement time is limited by the escape of plasma from the ends of the theta pinch coil. The escape velocity is about the ion thermal velocity parallel to the magentic field. The size of the effective escape hole was calculated using various models (l. c. [12–16]), and is mainly dependent on β, on the particle mean free path, and on the relative magnetic field strength at the coil ends. In hot theta pinch plasmas where the ion mean free path is long compared to the plasma dimensions, the size of the effective escape hole has been found experimentally to be of the order of an ion gyro radius [17, 5]. If attempts to reduce end losses should fail, a sufficiently close approach to the Lawson criterion using linear coils will only be possible with a length of several hundred meters at least.

In addition to the above problem, an important loss of energy occurs at the coil ends from heat conduction by (rapidly moving) electrons, since the plasma layer which extends along the field lines to the vessel walls provides effective thermal contact [18, 19]. Furthermore, the ends of the theta pinch may give rise to a rotation of the entire plasma column [20–22], and also to enhanced diffusion [23] of the plasma perpendicular to the magnetic field lines.

These end-effects of the open geometry can be avoided in a closed toroidal magnetic field configuration. A linear theta pinch coil can be transposed most simply to a toroidal geometry by retaining symmetry with respect to the centre plane ($z=0$) of the torus. This symmetry then also refers to the magnetic field configuration produced by the coil, and to the current distribution in the plasma. In a toroidal theta pinch where the coils form an axially symmetrical torus (i. e. a body of revolution), the field lines of the confining magnetic field are circles of radius R. In this case the magnetic field strengths along field lines close to the axis of symmetry ($R=0$), and hence also the magnetic pressure $B^2/2\,\mu_0$, exceed their values along field lines further away from the axis of symmetry. Thus in contrast to the linear theta pinch the plasma is no longer in equilibrium with the confining magnetic field [24], but is accelerated radially outward at every point in the direction of the (major) torus radius R. This acceleration, b_r, is proportional to the curvature of the torus, $1/R$, as well as to the sum of $k\,T_i$ and $k\,T_e$, and is independent of β [25–27].

In order to permit an equilibrium plasma position in such a toroidal theta pinch, the field lines situated closer to the symmetry axis ($R=0$) of the torus must be extended so as to reduce the field strength along these lines until it is equal to the field strength along the more remote field lines [28]. This condition can be explained using a $\beta=1$ model of the toroidal plasma, where the diamagnetic currents are assumed to flow along the surface of the plasma column [29, 30]. The equlibrium condition then leads to the requirement that the magnetic pressure $B^2/2\,\mu_0$ of the magnetic field tangent to the surface, should be equal to the plasma pressure p,

[11] L. Spitzer Jr., Physics of Fully Ionized Gases, Intersci. Publ., New York 1956.
[12] I. Berkowitz, K. O. Friedrichs, H. Goertzel, H. Grad, I.
[13] N. J. Phillips and I. K. Wright, J. Nucl. Energy, C, **1**, 240 [1960].
[14] K. V. Roberts, J. Nucl. Energy, KC, **1**, 243 [1960].
[15] J. A. Wesson, PPCNFR CN-21/43, Culham [1965].
[16] W. Grossmann Jr., Phys. Fluids **9**, 2478 [1966].
[17] W. E. Quinn, E. M. Little, F. L. Ribe, and G. A. Sawyer, Los Alamos Report LA-3487-MS [1966].
[18] H. A. B. Bodin, T. Green, A. A. Newton, G. Niblett, and J. Reynolds, PPCNFR, CN-21/34, Culham [1965].
[19] T. S. Green, D. L. Fisher, A. H. Gabriel, F. J. Morgan, and A. A. Newton, Phys. Fluids **10**, 1663 [1967]. Killeen, and E. Rubin, Proc. II. Genv. Conf. **31**, P/1538 [1958].
[20] H. A. B. Bodin and A. A. Newton, Phys. Fluids **6**, 1338 [1963].
[21] H. A. B. Bodin, J. McCartan, A. A. Newton, and G. H. Wolf, PPCNFR CN-24/K-1 Novosibirsk [1968].
[21a] PPCNFR CN-24/K-1 ... bedeutet: Plasma Physics and Controlled Nuclear Fusion Research, Conference Proceedings Novosibirsk 1968, Vienna 1969.
[22] M. G. Haines, Adv. Phys. **14**, 54, 164 [1965].
[23] R. L. Morse, Phys. Fluids **10**, 1560 [1967].
[24] L. Biermann u. A. Schlüter, Z. Naturforsch. **12 a**, 805 [1957].
[25] W. Lotz, F. Rau, E. Remy, and G. H. Wolf, Max-Planck-Institut für Physik und Astrophysik, München, Report MPI-PA-10/64 [1964].
[26] P. C. T. van der Laan, J. Nucl. Energy, C, **6**, 559 [1964].
[27] A. Schlüter, Institut für Plasmaphysik, Report, IPP 6/38 [1965].
[28] F. Meyer and H. U. Schmidt, Z. Naturforsch. **13 a**, 1005 [1958].
[29] R. Kippenhahn, Z. Naturforsch. **13 a**, 260 [1958].
[30] M. D. Kruskal and M. Schwarzschild, Proc. Roy. Soc. London A **223**, 348 [1954].

which is constant over the whole surface. Since $\oint B\,dl$ is constant along all field lines between the plasma column and the field coil, the field lines on the plasma surface must all be of equal length for the equilibrium condition to be fulfilled. Such toroidal plasma surfaces, usually referred to as M & S configurations, are therefore characterised by bulges which, because of the required constant length of the field lines, show the strongest amplitude of corrugation at those positions closest to the symmetry axis $R=0$.

From the practical point of view, however, it is not only important that any confinement scheme should fulfill the equilibrium condition for the plasma, at a given position, but also how sensitive it proves with respect to small displacements from this position, or small variations of the external boundary conditions, e. g. with the field coils. This is the question of the macroscopic stability [30–33] of a plasma in the configuration under discussion. If the magnetic field strength decreases with distance in an outward direction from certain areas of the plasma surface (associated with a concave curvature of the magnetic field lines), the equilibrium tends to become unstable [32]. Conversely, however, a field strength which increases with distance from the plasma surface (therefore associated with a convex curvature of the field lines), has a stabilizing effect.

In the case of a theta pinch of infinite length, the magnetic field lines have no curvature, and the plasma is in a state of marginal equilibrium. Conversely, toroidal M & S configurations characterised by periodic corrugations or bulges, include regions of both concave and convex curvature. Theoretically the modes and growth times of the instabilities [34–42] resulting from this geometry depend on the various plasma parameters and on the particular models used to describe them. Experimentally in a collision dominated plasma a displacement or kinking of the total plasma column was found [21] to limit the plasma confinement in agreement with the MHD-model. This $m=1$ instability is believed to be the most dangerous one also for collisionless bulged theta pinch plasmas in the characteristic range of beta. Due to this instability the confinement time in a static M & S system is not expected to overcome the toroidal drift time (in a purely azimuthal field) by more than an order of magnitude, as was found in previous M & S experiments in a low temperature regime. Efforts are made to suppress this instability by dynamical methods.

This report discusses some problems associated with the M & S configuration. The results of both theoretical and experimental investigations into the equilibrium and stability of the M & S configuration are reviewed.

2. Equilibrium

Let us assume that the magnetohydrodynamic model constitutes a suitable description of the macroscopic state of a hot theta pinch plasma following its rapid compression. Equilibrium between a fully ionized quiescent plasma having an isotropic pressure p, and the (confining) magnetic field $\boldsymbol{B}$ is given, according to SCHLÜTER [43], by

$$\nabla p = \boldsymbol{j} \times \boldsymbol{B} \tag{1}$$

(neglecting the effect of gravity). Scalar multiplication of Eq. (1) by $\boldsymbol{j}$ or $\boldsymbol{B}$ gives

$$\boldsymbol{j} \cdot \nabla p = \boldsymbol{B} \cdot \nabla p = 0\,, \tag{2}$$

i. e., the plasma pressure is constant both along the current lines $\boldsymbol{j}$ and along the magnetic field lines $\boldsymbol{B}$.

In toroidal equilibrium configurations, the magnetic field lines lie on nested toroidal surfaces of constant pressure in accordance with Eq. (2). When these isobar surfaces are ergodically covered by the field lines, one refers to "magnetic surfaces", the innermost of which for $\beta<1$ degenerates into a line

[31] K. HAIN, R. LÜST, and A. SCHLÜTER, Z. Naturforsch. **12 a**, 833 [1957].
[32] M. N. ROSENBLUTH and C. LONGMIRE, Ann. Physics **1**, 120 [1957].
[33] J. B. BERNSTEIN, E. A. FRIEMAN, M. D. KRUSKAL, and R. M. KULSRUD, Proc. Roy. Soc. Lond. A **244**, 17 [1958].
[34] H. WOBIG, Institut für Plasmaphysik, Report IPP 6/53 [1966].
[35] M. N. ROSENBLUTH, N. A. KRALL, and N. ROSTOKER, Nucl. Fus. Suppl. Part I, 143 [1962].
[36] D. PFIRSCH and H. WOBIG, PPCNFR, CN-21/55, Culham [1965].
[37] P. MERKEL and A. SCHLÜTER, Institut für Plasmaphysik, Report IPP 6/48 [1966].
[38] H. WOBIG, Proc. Eurat. Symp. Theor. Plasma Phys., Varenna, **I**, 135 [1966].
[39] F. HAAS and A. WESSON, Phys. Fluids **9**, 2472 [1966].
[40] R. L. MORSE, Phys. Fluids **10**, 236 [1967].
[41] H. WOBIG, Institut für Plasmaphysik, Report IPP 6/57 [1967].
[42] F. HAAS and A. WESSON, Phys. Fluids **10**, 2245 [1967].
[43] A. SCHLÜTER, Z. Naturforsch. **5 a**, 72 [1950].

which is then the magnetic axis. On the magnetic axis the plasma pressure has an extremum, as a rule a maximum. During one circuit of the field lines about the long (azimuthal) path of the toroidal isobar surface, they also cover, in general, a certain distance in the direction of the short (meridional) path. This characteristic is called a rotational transform.

To obtain a measure of the rotational transform t on an isobar surface, we follow a magnetic field line on this surface for a given distance and find the limiting value of the ratio of the number of circuits in the meridional direction Θ to the number of circuits in the azimuthal direction Φ,

$$t = \frac{\iota}{2\pi} = \lim_{\Phi \to \infty} \left(\frac{\Theta}{\Phi} \right). \tag{3}$$

An irrational value of t thus corresponds to an eregodically covered magnetic surface, whereas with a rational t all field lines on an isobar surface close on themselves after one or more azimuthal circuits.

In what follows we will only consider isobar surfaces with rational t, in particular with $t = 0$, but we allow these surfaces to have a periodicity along the magnetic field lines. With these restrictions NEWCOMB [44] and HAMADA [45] have shown that all magnetic field lines within the same isobar surface must have the same value of the integral

$$q = \int \mathrm{d}l/B \tag{4}$$

which is taken either over one of the above-mentioned periods, or along a (multiple) circuit of the field line back to its initial point.

Practical calculations of toroidal equilibrium surfaces having $t = 0$, i. e. M & S configurations, have been carried out thus far only for special simplified cases. Both the limiting case of $\beta = 0$ (i. e. the effect of plasma currents on the net confining magnetic field is neglected) and the case of arbitrary β, but with only plasma surface currents allowed have been treated. The existence of M & S configurations for arbitrary values of β and continuous radial pressure profiles has been proved recently by LORTZ [46].

A number of configurations having $\beta = 0$ were represented numerically by LORTZ and WELTER [46a] by the superposition of certain multipole field configurations upon a purely azimuthal magnetic field. An example of such a configuration is given in Fig. 1. Usind cylindrical coordinates (R, φ, z), a cross section is shown in the plane $z = 0$ and another cross section in the $\varphi = 0$, $\varphi = 2\pi/n$ plane; here n is the number of symmetry planes along φ, and $n/2$ thus gives the total number of periods of the configuration. In the example shown $n/2 = 24$.

A further parameter is the ratio of the azimuthal magnetic field to the total multipole field. The characteristic parameters given in Fig. 1 are $Q = q/q_0$, $B_{\mathrm{rel}} = B/B_0$, and $L = l/l_0$ ($l = \int \mathrm{d}l$ along a field line). The values of q_0, l_0, B_0 refer to the field line having the minimum value of q for the given configuration.

In the case of the toroidal theta pinch, we are interested here in particular in those configurations without rotational transform which have a high β region in the vicinity of the field line where the plasma pressure is maximum. In that case a more suitable approximation is to replace the pressure gradient at the plasma boundary with a pressure discontinuity Δp, and the diamagnetic currents with a surface current density $\boldsymbol{j}^*$. KRUSKAL and SCHWARTZSCHILD [30] have given the relevant equisibrium condition [Eq. (1)] in the modified form

$$\boldsymbol{j}^* \left(\frac{\boldsymbol{B}_\mathrm{i}^* + \boldsymbol{B}_\mathrm{a}^*}{2} \right) = -\boldsymbol{n}\, p \tag{5}$$

where

$$\boldsymbol{j}^* = \frac{1}{\mu_0} \boldsymbol{n} \cdot (\boldsymbol{B}_\mathrm{a}^* - \boldsymbol{B}_\mathrm{i}^*). \tag{6}$$

$\boldsymbol{n}$ is a unity vector in the outward normal direction from the surface of discontinuity and $\boldsymbol{B}_\mathrm{a}^*$ and $\boldsymbol{B}_\mathrm{i}^*$ are the limiting values of the magnetic field on the outside and inside respectively of the surface of discontinuity. Combining Eq. (5) and (6),

$$\Delta p = \frac{1}{2\mu_0} (B_\mathrm{a}^{*2} - B_\mathrm{i}^2). \tag{7}$$

With the simplifying assumption that $B_\mathrm{i}^* = 0$, it follows that

$$p = \frac{1}{2\mu_0} B_\mathrm{a}^{*2} = \frac{\mu_0}{2} j^{*2}. \tag{8}$$

Then Eq. (6) states that $\boldsymbol{B}_\mathrm{a}^*$ and $\boldsymbol{j}^*$ are orthogonal at every point on the boundary surface, and Eq. (8) that they are proportional. A constant value of surface current density means by definition that the

[44] W. A. NEWCOMB, Phys. Fluids **2**, 362 [1959].
[45] S. HAMADA, Nucl. Fusion **2**, 23 [1962].
[46] D. LORTZ, Institut für Plasmaphysik München-Garching, private communication [1969].
[46a] D. LORTZ and H. WELTER, Institut für Plasmaphysik München-Garching, private communication [1967].

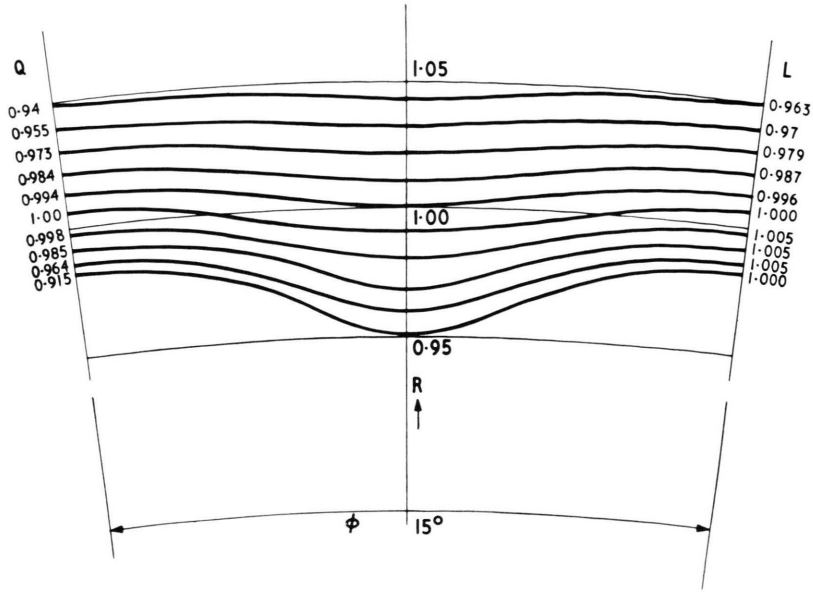

Fig. 1. Example of a $\beta=0$ M & S type magnetic field configuration [46a] using cylinder coordinate R, φ, z. The characteristic parameters are $Q=q/q_0$, $B_{\mathrm{rel}}=B/B_0$ and $L=l/l_0$ ($l=\int dl$ along the field lines). The values q_0, l_0 and $B_0=\int B\,\mathrm{d}l/l_0$ refer to the field line with the minimum value of q. (a) cross section in the $z=0$ plane, (b) cross section in a $\varphi=$const plane at the bulge; (c) cross section in a $\varphi=$const plane at the neck.

Fig. 1 a.

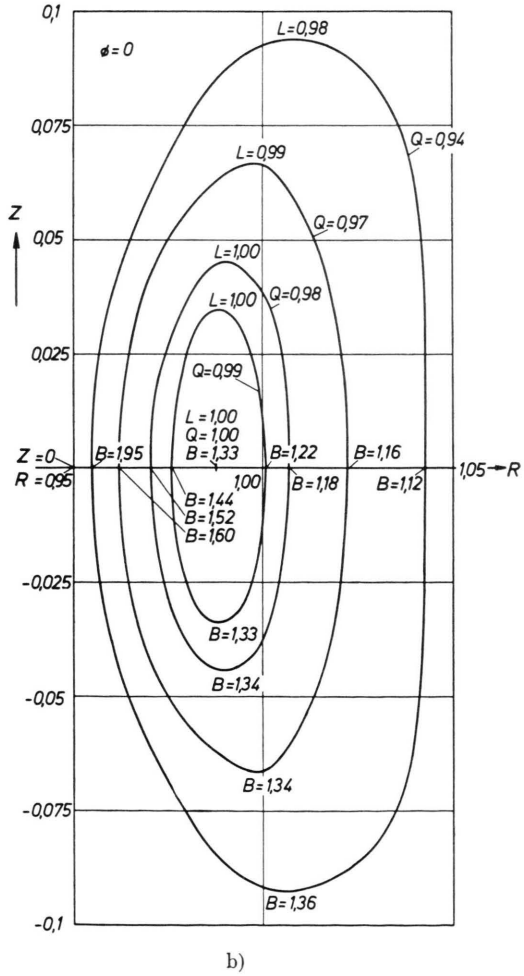

b)

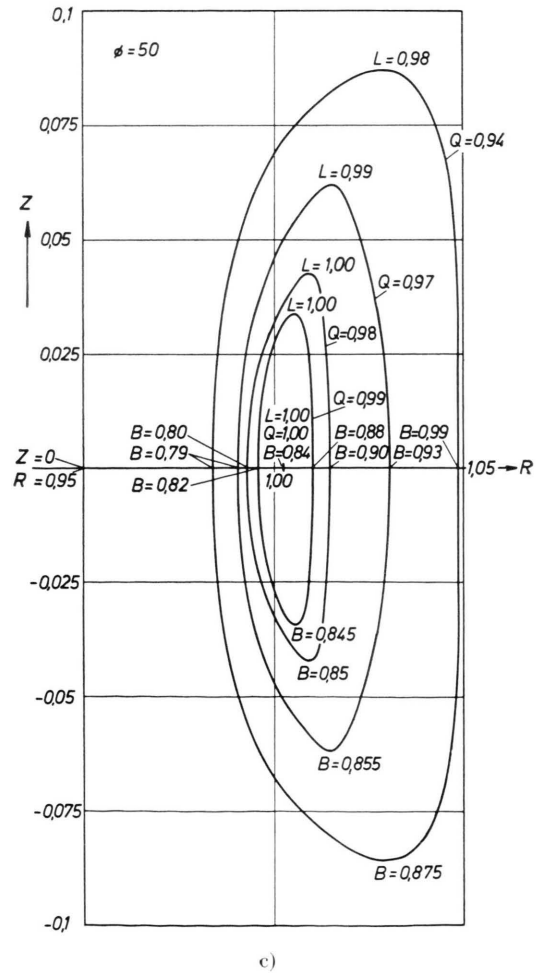

c)

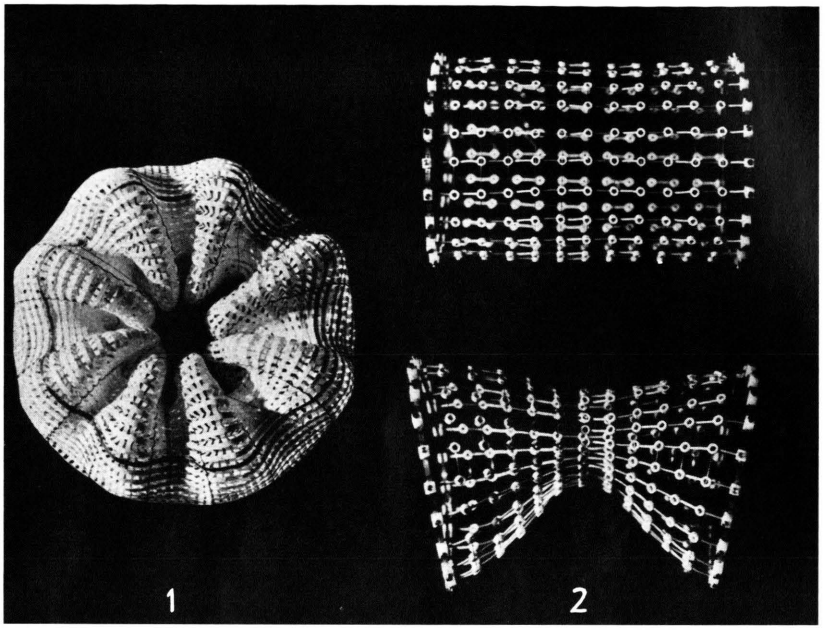

Fig. 2. Analogue model for representation of M & S surfaces. 1 — paper model [28]; 2 — wire model suggested by JUNKER.

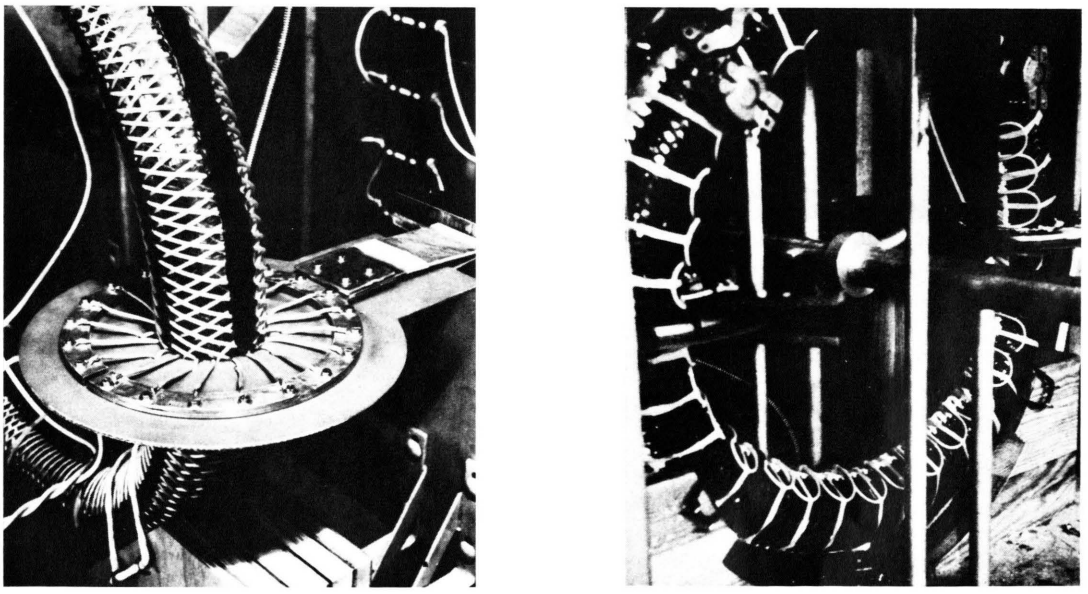

c) b)

Fig. 9. Coils to produce the B_q main field and the auxiliary field. (a) torus section and collector connection for B_q windings [64]; (b) auxiliary current windings [63].

[64] D. DIMOCK, U. GROSSMANN-DOERTH, W. LOTZ, E. REMY, and G. H. WOLF, Max-Planck-Institut für Physik und Astrophysik, München, Report MPI-PA-13/63 [1963].

current "lines" are equally spaced, from which it follows that, in the case of closed magnetic field lines in the surface, all field lines must be the same length.

Let us now consider the problem of approximating the surface current distribution j^* assumed in the above model by a real theta pinch plasma. LONGMIRE and ROSENBLUTH [47] have estimated the minimum thickness of the boundary layer between a collision-less, field-free plasma (neglecting for the moment this contradiction to the MHD model) and the confining magnetic field to be approximately $\sqrt{\varrho_e \varrho_i}$, where ϱ_e, ϱ_i are the electron and ion gyroradii respectively. For typical hot theta pinch plasmas this value is $\sim 10^{-2}$ cm, and is consequently smaller than the minimum plasma radius by two orders of magnitude. In fact, in the linear theta pinch experiments to be discussed, the formation of a boundary layer or plasma pressure gradient of at least the order of ϱ_i was always observed, which implies a bell-shaped rather than a box-type pressure profile. Theoretically the width of this larger boundary layer can be explained by end-effects [23] or by micro-instabilities *** occurring only during the early stages [21] of a theta pinch discharge.

According to Eqs. (6) and (8), it is necessary that the equilibrium surface of a plasma which contains no interior magnetic field be covered by a system of equidistant current lines free from singularities. That this requirement is also sufficient for the construction of special equilibrium configurations has been demonstrated by KIPPENHAHN [29]. The magnetic field lines $\boldsymbol{B}_a^*$ perpendicular to $\boldsymbol{j}^*$ are therefore geodetic lines [28, 29].

As mentioned earlier, we have been discussing the case of field configurations having symmetry about the plane $z=0$. In this case, in order to achieve equal length magnetic field lines over the whole surface, the surface must have (periodic) corrugations which show the strongest bulge in the direction of the axis, $R=0$. This becomes more evident by examining analog models, two of which are shown in Fig. 2 †. The first, due to MEYER and SCHMIDT [28], consists of a grid of paper strips. The larger, equilength strips represent magnetic field lines. The orthogonal hinged paper strips are of varying length but constant spacing, and thus satisfy the condition for the current lines. The second model was suggested by J. Junker and represents a mechanical variation of the first, in that equilength elastic wires (the field lines) are connected orthogonally at equal distances with variable length elastic wires (the current lines). A cylindrical segment and the corresponding toroidal segment of this model are shown. The wires corresponding to current lines can move freely within their junctions and the inflection points of the wire curves must be situated only on such mechanical intersections or junctions.

The first investigation into the existence and shape of M & S surfaces was carried out by MEYER and SCHMIDT [28], who considered the special case of non-parallel, planar current lines as shown in Fig. 3

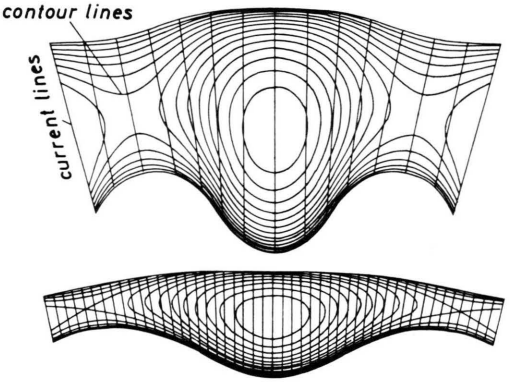

Fig. 3. Numerically calculated M & S surfaces in contour line representation. The equidistant current lines are located in planes perpendicular to the image plane.

in contour line representation. The aspect ratio, $A=\bar{r}_p/R_0$ ($\bar{r}_p$ is the mean plasma radius, R_0 the mean major torus radius) differs by about a factor 2.5 between the two cases. The total number of periods $n/2$ along the major torus circumference is 16.

The examples shown belong to a class of M & S surfaces wherein, for a fixed mean major torus radius R_0, the length of the magnetic field lines (and thus also their corrugation on the inner contour line in the $z=0$ plane) takes on a minimum value. The outer contour in this case represents the closest possible approximation to a circle; the circular shape itself is not allowed, however, for the special assumption of planar current paths [28].

As a better approximation to a real theta-pinch plasma, let us consider the M & S "surface" as the

[47] C. L. LONGMIRE, Elementary Plasma Physics, S. 95, Intersc. Publ., New York—London 1963.

*** See section 3.

† Fig. 2, 9, 10—13 on page 1002 a, b.

boundary sheath which divides the internal $\beta \approx 1$ plasma region from an external $\beta \ll 1$ plasma region surrounding the high β plasma. For the equilibrium condition to be fulfilled it then follows, that in the external $\beta \ll 1$ plasma regions closed nested q-surfaces must envelope the high β M & S plasma. Since the M & S surface is itself a q surface, surrounding adjacent q surfaces can exist only when, proceeding outward from any field line lying in the M & S surface, all δq have the same sign. The M & S field lines close to the torus axis ($R=0$) satisfy the condition $\delta q < 0$, according to Eq. (25) †.

Therefore the M & S surface must be so shaped that the criterion $\delta q < 0$ is satisfied on all field lines. It then also follows that, considering the M & S surface as fixed, the $\beta \ll 1$ plasma adjacent to this surface will be located in a magentic field which is stable with respect to interchange perturbations.

To investigate this problem, PFIRSCH and WOBIG [36] examined a further group of M & S surfaces, with $\beta = 1$, where the assumption of planar current paths is dropped. Starting from a reference circle $R = R_0$ in the $z=0$ plane, toroidal coordinates (r, φ, Θ) were used to construct an auxiliary torus $r_p(\varphi, \Theta)$ which coincides with rigorous M & S surfaces both along the inner and outer contour as well as around the periphery of the constricted and bulging regions. This auxiliary torus has the form

$$r_p(\varphi, \Theta) = r_H + b(\Theta)\, \frac{c}{2}\left(1 - \cos\frac{n}{2}\right)\varphi \qquad (9)$$

and a cross section in the $z=0$ plane is shown in Fig. 4. The function $b(\Theta)$ in Eq. (9) is specified [$b(\pi) = 1$] such that instead of the magnetic field lines, the lines $\Theta = \text{const}$ are of equal length. The auxiliary torus thus has periodic symmetry regions

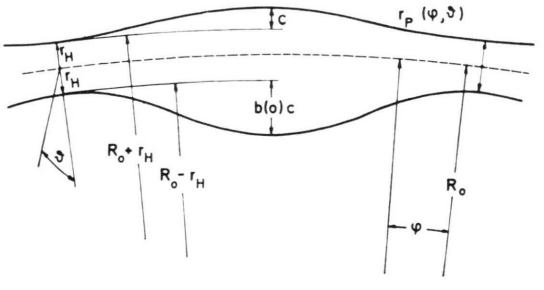

Fig. 4. M & S auxiliary torus given by Eq. (9). In the example shown, Eq. (25) is satisfied in addition. The special parameters are $R_0 = 100\, r_H$, $c = r_H$, $L = \pi R_0/18$ [34].

† See following section and Fig. 6.

given by

$$\varphi = \varphi_\nu \quad (\nu = 1, \ldots, n) \quad \text{with} \quad \frac{\partial r_p}{\partial \varphi} = 0. \qquad (10)$$

In this context we define the aspect ratio as

$$A = \frac{r_H}{R_0} \qquad (11)$$

With the limitation $A \ll 1$ and $\varepsilon \ll 1$ where

$$\varepsilon = 16\, R_0/n^2\, c \qquad (12)$$

it then follows that

$$b(\Theta) \approx 1 + \left(2\,\frac{r_H}{c} + 1\right)(1 + \cos\Theta)\,\varepsilon\,. \qquad (13)$$

It has been shown [34] that deviations between this M & S auxiliary torus, described by Eqs. (9) – (13) and the rigorous M & S surface are only of order A^2. For the case $c/R_0 \ll 1$, the criterion $\delta q < 0$ from Eq. (24) leads to the following additional constraint on the parameters of the auxiliary torus [36]:

$$\frac{1}{\varepsilon(1 + 2\, r_H/c)} \geqq 1\,. \qquad (14)$$

With the restriction $L \ll \sqrt{r_p R_0}$, Eq. (14) can be substituted in Eq. (12) to give

$$c/2 \gtrsim \frac{L}{\pi\sqrt{2}}\sqrt{\frac{r_H}{R_0}}\,. \qquad (15)$$

Using Eq. (13) we obtain for the maximum amplitude of the corrugation in that case

$$b(\Theta = 0)\; c/2 \approx \frac{3\,L}{\pi\sqrt{2}}\sqrt{\frac{r_H}{R_0}}\,. \qquad (16)$$

When looking for the weakest possible M & S corrugation we choose a configuration with a circular outside contour, i. e. $b(\pi) = 0$. Then, from the equal length condition, we obtain the smallest value of the maximum corrugation amplitude

$$b(\Theta = 0)\; c/2 = \frac{\sqrt{2}\,L}{\pi}\sqrt{\frac{r_H}{R_0}}\,. \qquad (17)$$

M & S configurations with surface currents extended to the $\beta < 1$ case were recently represented by JOHNSON, MORSE and RIESENFELD [48], who included the confining magnetic field as well as the current distribution setting up this magnetic field. For the plasma radius $r_p(\varphi, \Theta)$ the following expression was assumed

$$r_p(\varphi, \Theta) = \bar{r}_p\{1 + \delta(\varphi, \Theta)\} \qquad (18)$$

[48] J. L. JOHNSON, R. L. MORSE, and W. B. RIESENFELD, Plasma Physics **10**, 543 [1968].

where

$$\delta(\varphi, \Theta) = \sum_{l=0}^{\infty} \delta_l \cos l\,\Theta \sin k\,\varphi. \qquad (19)$$

With the realistic assumption $A \ll 1$ and $L \gg \bar{r}_p$ a relationship is established between the δ_l, β and the dimensions of the bulge. A series expansion from this relation with the ordering parameter

$$\varepsilon = \frac{2\,L^2}{(3-2\,\beta)\,4\,\pi^2\,\bar{r}_p\,R_0\,\delta_0^2} \qquad (20)$$

gives, for example to third order, the following solution [48]

$$\begin{aligned} \frac{\delta_1}{\delta_0} &= \varepsilon \left\{1 + \frac{\beta\,\varepsilon^2}{2(3-2\,\beta)}\right\}, \\ \frac{\delta_2}{\delta_0} &= -\frac{\beta\,\varepsilon^2}{4(2-\beta)}, \\ \frac{\delta_3}{\delta_0} &= \frac{3\,\beta^2\,\varepsilon^2}{8(2-\beta)\,(5-2\,\beta)}. \end{aligned} \qquad (21)$$

The convergence of that series is shown for $\varepsilon \lesssim 1$.

For the $\beta = 0$ case Eq. (21) yields a circular outside contour with $\delta_0 = \delta_1$ $(\varepsilon = 1)$. The maximum corrugation amplitude then becomes

$$(\delta_0 + \delta_1)\,\bar{r}_p \approx \frac{L}{\pi}\sqrt{\frac{2\,\bar{r}_p}{3\,R_0}} \qquad (17\,a)$$

thus being a factor of $\sqrt{3}$ smaller than for the $\beta = 1$ case from Eq. (17). For $\beta = 0.5$ this factor becomes about $\sqrt{2}$. KEMP, QUINN, RIBE and SAWYER [49] have published graphs of the ratios δ_0/δ_1 and δ_0/δ_2 as a function of δ_0 for the cases $\beta = 1$, and $\beta = 0.75$; they also show a coil element intended to produce the $l = 1$ component of an M & S magnetic field.

General M & S configurations for the diffuse (bell-shaped) pressure profiles found in real theta pinch plasmas, although proved to exist [46], have not yet been calculated. Theoretical results on this subject are confined to the simpler two-dimensional problem of the linear theta pinch having periodic corrugations. MERKEL and SCHLÜTER [37] have treated this configuration and their results have been compared with the LIMPUS experiment discussed below. Fig. 5 shows the field lines for a bell-shaped pressure profile (see curve HB in Fig. 21) with $\beta = 1$ on the axis of the bulge. It is typical of such a configuration that with increasing radial distance from the plasma column the corrugation of the field lines remains at first approximately

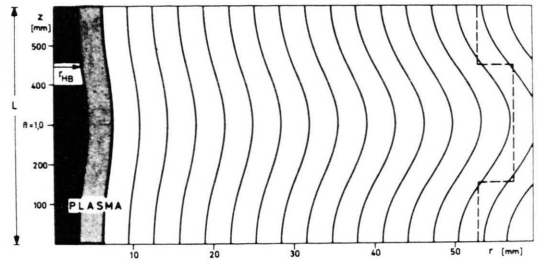

Fig. 5. Magnetic field configuration of a corrugated theta pinch plasma with $\beta_{max} = 1$ and bell-shaped pressure profile according to the line HB in Fig. 21. The "neck" and "bulge" radii of the sinusoidally corrugated isobar surface $p = p_{max}/2$ agree with the half width of the curves H and B in Fig. 21; the drawn-in mean plasma radius r_{HB} corresponds to the half width of the curve HB. The dashed line shows the region of the coil used for the Garching LIMPUS experiment [50].

unchanged, but then increases such that near the vessel wall the corrugation is stronger than in the plasma. This latter effect increases as β_{max} decreases [37], so that the shape of the magnetic field at any given position gradually approaches that of the vacuum magnetic field of a corrugated theta pinch coil, as the reaction of the diamagnetic plasma currents on the confining magnetic field declines. It thus appears that for a given linear coil surface (a flux tube) which does not change with time, the initial corrugation of the plasma column is smoothed out if during a discharge the initially steep pressure profile relaxes and the initially high value of β_{max} (see Fig. 14 b) drops. Finally let us return to the question of the closed nested q-surfaces outside the region of high β. When using the condition of Eq. (14) it is postulated that everywhere $\delta q < 0$. For the specified type of field configuration this can

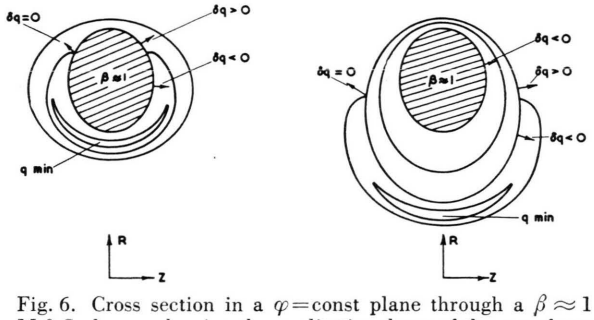

Fig. 6. Cross section in a $\varphi = \text{const}$ plane through a $\beta \approx 1$ M & S plasma, showing the qualitative shape of the q-surfaces surrounding the plasma column. Left hand side: criterion of Eq. (14) not fulfilled; right hand side: criterion of Eq. (14) fulfilled.

[49] E. L. KEMP, W. E. QUINN, F. L. RIBE, and G. A. SAWYER, Proc. Los Alamos Conf. [1967].

[50] C. ANDELFINGER, G. DECKER, E. FÜNFER, E. REMY, M. ULRICH, H. WOBIG, and G. H. WOLF, Institut für Plasmaphysik, München-Garching, Report IPP 1/55 [1966].

only be fulfilled if β is sufficiently close to unity and if $\bigtriangledown p$ is sufficiently large. Even then, at a certain distance from the high-β M & S surface, there is a $q = \text{const}$ surface on which δq changes sign and which consequently has two branching points at $\delta q = 0$, leading to the formation of an "island" as shown schematically in Fig. 6. This is avoided by a configuration where $\delta q > 0$ everywhere, which is the case for a sufficiently gentle $\bigtriangledown p$. From the above mentioned calculations using a diffuse bell-shaped profile, it can be estimated that for $A \ll 1$, L in the region $10 - 30$ cm, and r_p in the region $0.5 - 1$ cm, one has $\delta q > 0$ everywhere when $\beta_{max} \leqq 0.6$. This regime corresponds more closely to future experiments in theta pinches [49].

3. Stability

We will consider in this section only those stability problems which arise from the geometrical requirements for toroidal equilibrium, and which therefore do not occur in infinitely long linear theta pinches.

This consideration excludes the class of microinstabilities (e. g. [51–53]) and the related anomalous diffusion of plasma across the confining magnetic field. As mentioned earlier, microinstabilities are due to a sufficiently large departure from the microscopic thermal equilibrium distribution. Such departures can arise in the linear theta pinch, e. g., from end losses, from the pressure gradient necessary for confinement, or from the input of directed energy during the fast compression stage.

Although an anisotropy of the velocity distribution due to the end loses is no longer relevant in the toroidal theta pinch, posible perturbations by the diamagnetic currents or by the fast compression will be comparable with the linear geometry. To those must be added the forces arising from the curved magnetic fields which, in regions of unfavourable curvature, act on the particles in a direction outward from the plasma axis. To simplify the problem, these forces are usually simulated by a "gravitational acceleration" term which, when the gyro-radii may be considered negligibly small [51], leads to the instabilities occuring also in the macroscopic MHD model. Consideration of finite (nonzero) gyro-radii even can introduce a stabilising influence.

Primarily dangerous in going over to the toroidal theta pinch are thus the macroscopic MHD instabilities, subject possibly to the stabilising influence of finite gyro-radii effects. This is experimentally supported by the fact that observations in a collision dominated theta pinch plasma for times long compared with the relevant MHD instability growth times have shown no anomalous diffusion following the fast compression stage [54, 21].

The characteristic property of the M & S configuration, compared with the normal linear theta pinch, is the corrugation of the plasma column which, seen from the plasma, gives alternating regions of decreasing (unfavourable curvature) and increasing (favourable curvature) magnetic field. The relative importance of the regions of unfavourable curvature, compared to those of favourable curvature, increases (because of the curvature of the torus) as the major torus radius R (for a given R_0) increases, or as the meridianal angle Θ increases (see Fig. 4).

Since the investigation of the stability properties of an M & S configuration presents considerable difficulties because of the complex shape, it is useful to consider first the simplified case of a periodically corrugated linear (axial-symmetric) theta pinch, often referred to as LIMPUS [55, 50]. Such configurations have been theoretically investigated using the ideal (infinite conductivity) MHD model [34, 36–39, 41, 42] and the so-called "bouncing" model [40, 17].

In the MHD model we start with an equilibrium configuration satisfying Eqs. (1) and (4), which is then perturbed. Any perturbations which decrease the net potential energy W of the plasma and its confining magnetic field will lead to instability. The stability criterion is thus given by

$$\delta W > 0 . \qquad (22)$$

[51] M. N. Rosenbluth, Plasma Physics, p. 485, IAEA Wien 1965.

[52] D. Pfirsch, Max-Planck-Institut für Physik und Astrophysik, München, Report MPI-PA 8/64 [1964].

[53] N. A. Krall u. M. N. Rosenbluth, Phys. Fluids **6**, 254 [1963].

[54] H. A. B. Bodin and A. A. Newton, Proc. Los Alamos Conference [1967].

[55] W. Lotz, F. Rau, E. Remy, and G. H. Wolf, Experiment LIMPUS — Parameter und Abschätzungen, Max-Planck-Institut für Physik und Astrophysik, München, internal report [1965] and annual report [1964]. The relevance of such an experiment for the M&S stability was first pointed out 1964 by D. Pfirsch, Institut für Plasmaphysik, München-Garching.

Consider once more the simplified case of a $\beta = 1$ plasma having only surface currents. Then, according to BERNSTEIN, FRIEMAN, KRUSKAL an KULSRUD [33], the variation δW of the total energy W can be split up into three terms

$$\delta W = \delta W_P + \delta W_F + \delta W_M \qquad (23)$$

where P is the plasma volume, F the plasma surface, M the external magnetic field. PFIRSCH and WOBIG [36] examined the special case where only $\delta W_F \neq 0$, since δW_P and δW_M always give a positive (hence stabilising) contribution if different from zero. In this special case the following criterion is valid

$$\delta W_F = \int \frac{\mu}{\varrho_n} \, dl > 0 \qquad (24)$$

where the integration is along the magnetic field lines in F, μ^{-1} is the distance between two field lines in a surface $p = \text{const}$, and $\varrho_n{}^{-1}$ the normal curvature of the field lines in the surface. For a $\beta \ll 1$ plasma variations of the potential energy W_M of the magnetic field cannot occur, and the energy variation δW associated with an interchange of two infinitesimally small flux tubes is thus given by $\delta W = \delta q$ [32] where q is defined by Eq. (4). One then has $\delta q < 0$ for the stability criterion with respect to such "interchange perturbations" for $\beta \ll 1$ plasmas. There is an analogy between this criterion and Eq. (24) based on the relation [36]

$$\delta q = - \int \frac{\mu}{\varrho_n B^2} \, dl \qquad (25)$$

which for the case $B^2 = \text{const}$ reverts directly-to Eq. (24). This means that when the criterion of Eq. (24) is satisfied for a $\beta = 1$ surface, stability with respect to interchange perturbations is then also guaranteed in adjacent external plasma regions where $\beta \ll 1$.

A sinusoidally corrugated linear plasma column having surface currents with $\beta = 1$ is described by the equation

$$r_p(z) = \bar{r}_p + a \cos k z \qquad (26)$$

where $L = 2\pi k^{-1}$ is the spatial wave length. In Fig. 7 such a LIMPUS plasma (mean radius $\bar{r}_p$) is shown schematically together with the coil (mean radius r_0) producing the confining magnetic field.

In this geometry Eq. (25) becomes [32]

$$\delta W_F = - \delta q = \int \frac{dl}{r_p \varrho_n B^2} > 0 \, . \qquad (27)$$

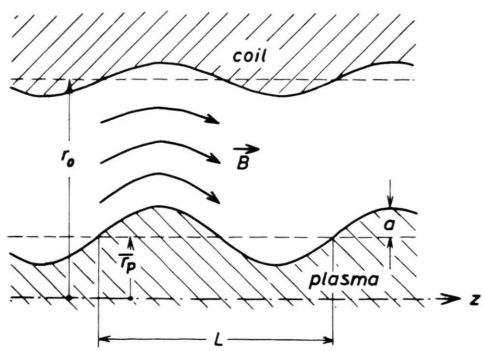

Fig. 7. $\beta = 1$ LIMPUS plasma according to Eq. (26), with mean radius $\bar{r}_p$ and corresponding magnetic field coil with mean radius r_0.

Since r_p is smaller in the regions of favourable curvature than in the regions of unfavourable curvature, and since by symmetry the shape of ϱ_n has the same weighting in either region, such a configuration ($B^2 = \text{const}$) is statble with respect to the above mentioned perturbations. An M & S surface according to Eq. (9) is also statble with respect to these specific perturbations, provided the criterion of Eq. (14) is satisfied simultaneously [36]. An analytical example of a LIMPUS surface perturbation ξ_n which satisfied Eq. (25) and the condition $\delta W_P = \delta W_M = 0$ is given by

$$\xi_n = \xi_0 \frac{1}{r_p(z)} \sin m \Theta \qquad (28)$$

where the angle Θ is designated by analogy to the M & S configuration. The perturbation ξ_n in Eq. (28) represents grooves parallel to field lines whose depth at a "neck" $[r_p(z) = \bar{r}_p - a]$ is larger than at a "bulge" $[r_p(z) = \bar{r}_p + a]$. To examine further stability characteristics, WOBIG [36] and HAAS and WESSON [39] have extended the stability investigation to the more general case with $\delta W_M \neq 0$. To calculate δW_M in this case, one assumes infinite conductivity of the internal coil surface (magnetic flux tube) with mean radius r_0 (Fig. 7). Since $\delta W_M > 0$, the stability condition becomes $\delta W_M / \delta W_F > 1$. For the following perturbations as test functions [34]

$$\xi_n = \xi_0 \sin m \Theta \qquad (29)$$

and

$$\xi_n = \xi_0 \sin m \Theta \cos \frac{k z}{2} \qquad (30)$$

this condition leads to the criterion [34, 39]

$$\frac{Q}{m} > 1 \qquad (31)$$

and $$\frac{Q}{m} \cdot \frac{\bar{r}_p^2}{a\,\bar{r}_p + a^2} > 1 \qquad (32)$$

respectively, where Q is defined in terms of r_0:

$$Q = \frac{1+(r_p/r_0)^{2m}}{1-(r_p/r_0)^{2m}}. \qquad (33)$$

The above equations show that since $(\bar{r}_p/r_0)^2 \ll 1$, all perturbations with $m \geqq 2$ lead to instability. HAAS and WESSON [42] have extended the model with surface currents to the case $\beta < 1$ (not $\beta \ll 1$) with a particular view to the $m = 1$ perturbations, and have thus obtained an improved approximation to real theta pinch plasmas. It was shown by these authors that below a critical value β_K (given a sufficiently weak corrugation, β may be assumed constant within the plasma volume) instability occurs even with respect to the $m = 1$ perturbations; β_K has the value

$$\beta_K = 1 - (r_p/r_0)^{2m}. \qquad (34)$$

The ratio $\bar{r}_p/r_0$ for hot theta pinch plasmas is approximately 1/10, so according to Eq. (34) $\beta_K = 0.99$. This value of β is unrealistically high for practical attainment in a weakly corrugated theta pinch plasma column, implying that the $m = 1$ perturbations are unstable as well.

An investigation of the MHD stability of a weakly corrugated straight plasma column having a diffuse radial pressure distribution has been carried out by WOBIG [41] concerning the higher ($m \gg 1$) modes. The field lines in the plasma were assumed to have the form

$$r(z) = \bar{r} + a(\bar{r}) \cos k z, \qquad (35)$$

where, because of the weak corrugation, $k a \ll 1$ and $a/\bar{r} \ll 1$. The stabilising effect of the inner coil surface was neglected. This model represents the best approach in describing a real theta pinch plasma; it also predicts that the LIMPUS configuration is unstable. Application of the variational principle yields the perturbation ξ_n for which δW assumes the maximum negative value; ξ_n has the shape [41]

$$\xi_n = \xi_0 \left[1 + a\left(\frac{2\mu_0 p'}{B_{\bar{r}}^2} - \frac{1}{\bar{r}}\right)\cos k z\right] \sin m\Theta \qquad (36)$$

where $B_{\bar{r}}$ is the magnetic field strength and $p' = \partial B/\partial r$ in the region of $\bar{r}$. In addition to the above limitations it was assumed in Eq. (36) that

$$\frac{2\mu_0 p' a}{B_{\bar{r}}^2} \ll 1. \qquad (37)$$

HAAS and WESSON [42] considered also the $m = 1$ instability for a diffuse pressure profile, described by the radial distribution of $B(z)$:

$$B(z) = B(z)_0 + \{B(z)_{r_p} - B(z)_0\}\left(\frac{r}{r_p}\right)^n \qquad (38)$$

where n is an even positive integer and $r < r_p$. The suffixes refer to the given value of r, the nought indicates the value on the axis. Using the instability test funciton of Eq. (29), the stability criterion with respect to $m = 1$ perturbations is [42]:

$$\frac{r_p}{r_0} < \left\{\frac{1-\beta_0 + \frac{2}{n}\sqrt{1-\beta_0}}{\beta_0}\right\} \qquad (39)$$

where r_0 is as usual the mean coil radius. For $r_p/r_0 \approx 0.2$, this leads to instability if $\beta_0 \lessapprox 0.97$.

By analogy to the investigations using the MHD model with surface currents and $\beta = 1$, MORSE [40] has calculated the LIMPUS stability using the so-called "bounce" model. In this model the plasma is treated as a collisionless gas whose particles are reflected at the sharp interface between plasma and magnetic field and move along straight trajectories in the interior. To satisfy this assumption, while allowing a sufficiently high temperature for the collisionsless approximation, the magnetic field strength B_i inside the plasma must be sufficiently small for the local gyro-radii of the ions at least to exceed the plasma radius r_p. We then obtain the following inequality for the validity of the "bounce" model, where ϱ_i is the ion gyro-radius outside the interface.

$$\beta > 1 - (\varrho_i/\bar{r}_p)^2. \qquad (40)$$

For practical calculations, Eq. (40) can be rewritten by expressing ϱ_i (in the case of position-independent temperatures) by the following equation (quantitative for D^+ ions):

$$\varrho_i \approx 3 \cdot 10^7 \sqrt{\frac{\beta}{n(1+T_e/T_i)}}\ (\mathrm{cm}). \qquad (41)$$

Combining Eqs. (41) and (40) yields

$$\beta > \frac{1}{10^{15}/n\,\bar{r}_p^2 + 1}\ (\text{dimensions cm}) \qquad (42)$$

where we have assumed $T_i \gg T_e$, a condition which is generally satisfied in a hot theta pinch plasma [5, 6]. Characteristic parameters would be $r_p = 0.5$ cm and $n = 2 \times 10^{16}\ \mathrm{cm}^{-3}$, giving $\beta > 0.8$. The practical realization of Eq. (42) thus is not assured. It is noteworthy however, that the results of the "bounce" model calculations, apart from the growth rates, agree essentially with the results from the MHD model. One again obtains that the LIMPUS configu-

ration is stable with respect to $m = 1$ perturbations because of the presence of a conducting coil surface ($m = 1$ stability is otherwise marginal) whereas perturbations for $m \geqq 2$ will grow unstable. In the approximation $2\,m\,a/r_p \ll 1$, the perturbation with the shortest growth time (i. e. the most unstable perturbation) has the following form [40]

$$\xi = \xi_0 \left[1 + \frac{a}{r_p}\,(m-1)\,\cos k\,z\right] \sin m\,\Theta, \qquad (43)$$

where again a sinusoidally corrugated equilibrium plasma surface, given by Eq. (26) has been assumed. The "most unstable" perturbation given by Eq. (43) agrees, for $m \gg 1$, with the most unstable perturbation in the MHD model [Eq. (36)] when $1/\bar{r} \gg 2\,\mu_0\,p'/B_r^2$. The results of stability calculations carried out thus far are summarized in the following table

The various models show strong variations in the growth times τ of the indicated instabilities. For the perturbation given by Eq. (29) and the corresponding $\beta = 1$ surface current model, one obtains the MHD growth time τ_s [34]

$$\tau_s = \frac{L}{\pi\sqrt{2}\,v_A\,\delta\sqrt{m-1}} \qquad (44)$$

where v_A is the Alfven velocity when for the value of the magnetic field there B_a is taken, and $\delta = a/\bar{r}_p$.

The growth time τ_B [of the perturbation given by Eq. (43)] for the analogous $\beta = 1$ "bounce" model is considerably longer [40, 17]

$$\text{for small } m \qquad \tau_B = \frac{L^2}{\pi^{5/2}\,v_i\,\delta^2(m-1)\,r_p} \qquad (45)$$

$$\text{for large } m \qquad \tau_B = \frac{L^2}{2\,\pi^{5/2}\,v_i\,\delta r_p}.$$

An estimate of the MHD growth time, $\tau_{m=1}$, according to the $\beta < 1$ surface current model, leads to [42]

$$\tau_{m=1} = \frac{L}{\sqrt{2}\,\pi\,v_A\,\delta}\left[\frac{1-\beta+Q}{\beta(3-2\beta)\{1+(1-2\beta)\,Q\}}\right]^{1/2}. \qquad (47)$$

For $Q \approx 1$ and $0.7 \gtrsim \beta \gtrsim 0.4$ this gives

$$\tau_{m=1} \approx L/\sqrt{2}\,\pi\,v_A\,\delta. \qquad (48)$$

Thus $\tau_{m=1}$ agrees with τ_s [Eq. (44)] for $m = 2$.

The growth time τ_v obtained from the volume current model is considered to be the most relevant one, in particular for the higher mode numbers. As an example consider the pressure distribution

$$p(r) = p_{max}\exp\{-(r/\bar{r}_p)^\alpha\} \qquad (49)$$

which yields a Gaussian profile for $\alpha = 2$. Then for $m \gg 1$ the corresponding growth time becomes independent of m [41]

$$\tau_v = \frac{L}{2\sqrt{3}\,v_i\,\delta}. \qquad (50)$$

To illustrate the growth times given by Eqs. (45) to (50), the diagram of Fig. 8 shows these times as

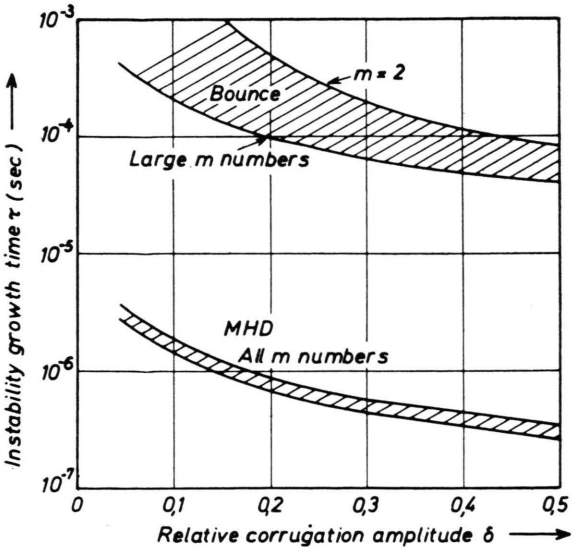

Fig. 8. Instability growth times according to Eqs. (45) — (50) as a function of the relative corrugation amplitude $\delta = a/\bar{r}_p$. The parameters of the sinusoidally corrugated LIMPUS configuration are $\bar{r}_p \approx 0.5$ cm, $L = 30$ cm and $v_i \approx v_A \approx 5 \cdot 10^7$ cm/sec ($k\,T_i \approx 3$ keV).

Model Pressure Distribution	MHD	MHD	MHD	bounce
β	1	<1	<1	1
$m = 2$	unstable [34, 42] $\tau_s \ldots 44$	unstable [42] $\beta < \beta_k \ldots 34$	unstable [41, 37] $\tau_v \ldots 50$	unstable [40] $\tau_B \ldots 45/46$
$m = 1$	stable [34, 42]	unstable [42] $\beta < \beta_k$ $\tau_{m=1} \ldots 47$	unstable [42]	stable [40]

Table 1. Results of stability calculations for the LIMPUS configuration. The appropriate reference is given in each case. The growth times τ are marked by the numbers of the corresponding equations given in the present paper.

a function of $\delta = a/\bar{r}_p$, assuming an experimentally relevant LIMPUS configuration with a sinusoidal corrugation of amplitude a, $\bar{r}_p \approx 0.5$ cm, $L = 30$ cm and $v_i \approx v_A \approx 5 \cdot 10^7$ cm/sec ($kT_i \approx 3$ keV). A plasma surface having a different axial variation behaves equivalent to a sinusoidally shaped one, if $\int (dr_p/dz)^2 dz$, taken over one period, remains unchanged [42].

From Fig. 8 it can be seen, that the MHD growth times, which are insensitive to m, are roughly of the order of one microsecond. Subsequently a very unfavourable picture is obtained regarding the possibilities of long term plasma confinement ($\gtrsim 10^{-2}$ sec) by means of an M & S configuration, unless these instabilities can be suppressed or their growth rates decesively reduced by additional measures.

As far as the $m \geqq 2$ perturbations are concerned a stabilising mechanism has been suggested based on the fact that in the theta pinch plasmas under discussion the ion gyro-radii are no longer small compared with the plasma radius. According to ROSENBLUTH, KRALL and ROSTOKER [35], the validity of stability investigations using the MHD model is questionable whenever

$$\tau \Omega_i \approx \left(\frac{\lambda}{2\pi \varrho_i}\right)^2 \tag{51}$$

where λ is the wavelength of the perturbation perpendicular to the magnetic field (in our case $2\pi\bar{r}/m$) and Ω_i is the ion gyro frequency. These authors considered some specific examples in which they showed that, in the approximation $\beta \ll 1$, the MHD unstable perturbations do not grow (in the collisionless case) provided the left-hand side of Eq. (51) is larger than the right-hand side.

The application of the criterion of Eq. (51) to thet LIMPUS configuration appears meaningful if the smallest gyro-radii existing in the outer regions of the plasma column ($\beta \ll 1$), as given by Eq. (41), are used instead of the relatively large ones. Substituting the growth time τ_s [Eq. (44)] into Eq. (51), the stability criterion for $m \geqq 2$ is found:

$$L \gtrsim \delta r_p^2/\varrho_i \tag{52}$$

which is likely to be satisfied for all LIMPUS configurations of interest. Even if the suppression of the $m \geqq 2$ instabilities remains incomplete, however, the damping of these modes will be sufficient for their growth times to exceed that of the $m = 1$ mode. Since it is not expected that similar damping mechanisms, e. g. increased viscosity due to ion-ion collisions, will significantly reduce the growth rate of the $m = 1$ mode, this instability is considered to be the most dangerous one in limiting the confinement time in any bulged theta pinch plasma.

The last stability question we have to consider concerns the extensions of the stability results obtained on the linear LIMPUS configuration to an appropriate toroidal M & S configuration. WOBIG [34] has shown that a torus whose major radius is large compared to all other dimensions in the problem does not involve a substantial variation of the stability characteristics from those of a linear system. For practical applications, however, we are interested in the M & S configuration with equivalent stability properties, which has the smallest major radius R_0. Although other choices are possible [56], we shall assume that the required equality is given when the maximum relative corrugation amplitude δ, the mean plasma radius r_p and the period length L remain the same. From Eq. (21), we then obtain an estimate of the minimum major torus radius R_0.

$$R_0 \gtrsim \frac{2}{\pi^2} \frac{L^2}{\delta^2 r_p}. \tag{53}$$

Having an estimate of R_0, we can examine the relationship between the containment times of both an M & S type torus and a smooth uncorrugated torus, assuming that the linear stability theory can be applied to perturbation amplitudes ξ growing up to dimensions of the order of the minor vessel radius. For this purpose we compare the instability growth time $\tau_{M\&S}$ (for an initial perturbation ξ_0 to grow by a factor of e) with the toroidal drift time τ_D (for a smooth plasma column confined by a purely azimuthal field, after having moved an initial distance ξ_0 from its starting position $v_0 = 0$, $R = R_0$, to move an additional distance $\xi_0(e-1)$ towards the wall]. This toroidal drift time is approximately given by [25, 26, 57–59] $\tau_D \approx 0.65 \sqrt{\xi_0 R_0}/v_i$; from Eq. (48) we get $\tau_{M\&S} \approx L/\sqrt{2}\pi v_i \delta$. Substituting these relations into Eq. (53) yields

$$\frac{\tau_{M\&S}}{\tau_D} \approx \sqrt{\frac{r_p}{\xi_0}}. \tag{54}$$

[56] G. H. WOLF, Institut für Plasmaphysik, Report IPP 1/63 [1967].

[57] J. JUNKER, Phys. Fluids **11**, 646 [1968].

[58] A. SCHLÜTER, Institut für Plasmaphysik, München-Garching, Report IPP 6/39 [1965].

[59] E. REMY, Max-Planck-Institut für Physik und Astrophysik, München, Report MPI-PA-62/1 [1962].

To use this relation we need an assumption about the amplitude ξ_0 of the initial deviation from the equilibrium, which may be already produced during the rapid compression phase of the discharge. For a rather optimistic appraisal, taking $\xi_0 \approx r_p/10$, we find $\tau_{M\&S}/\tau_D \approx 3$.

4. Toroidal M&S Experiments

The experiments described in this section were intended to demonstrate whether or not a high β M & S configuration can be set up or approximated adequately by using the theta-pinch approach.

An estimate based on Eq. (54) shows that in order to obtatin a markedly longer containment time than with a purely azimuthal magnetic field, the initial perturbation ξ_0 of the equilibrium position must be kept as small as possible.

To prevent undesirable axial movement of the plasma during the fast Θ-pinch compression, this condition requires that the length of the M & S period be large compared to the radius of the plasma column, which according to Eq. (52) is also desirable for FLR (finite Larmor radius stabilization). The major torus radius R_0 is then at least of the order of a few metres. For a mean minor coil radius of $r_0 = 5$ cm and a maximum magnetic field of $B_{max} = 100$ kG the magnetic field energy stored in the coil is $E_M = 1/3\, M J/m$; to operate a corresponding torus of $R_0 = 2$ m, a capacitor bank of 8 MJ is required (matching of about 50%). To avoid such an expense for the present let us consider some less ambitious methods of investigating M & S plasmas:

1. We may investigate the plasma behaviour at lower temperatures and correspondingly smaller confining magnetic fields. The gyro-radii remain of the same order [proportional to β/n; see Eq. (41)] whereas the mean free paths are reduced; e. g. at $n = 10^{16}$ cm^{-3}, the ion m.f.p. is reduced from about 100 m (at 3 keV) to 10 cm (at 10 eV). The increased collision frequencies which result lead to a strong increase of classical diffusion perpendicular to the confining magnetic field. The diffusion velocity of a 10 eV plasma having $\bar{r} = 0.5$ cm ($\bar{r}$ is the half width of the pressure profile) and $\beta = 1$ at the axis is of the order of $v_D \cong 3$ mm/μs assuming $\nabla p \cong p_{max}/2\,\bar{r}$. For such large v_D, the behaviour of high β plasmas in this temperature region can be observed only during the first few microseconds after the end of the fast compression.

2. We may reduce the torus radius R_0. This leads to stronger overall curvatures of the M & S surface and decreases the influence of FLR, thus $m \geqq 2$ perturbations may be expected in addition to the possible $m = 1$ instabilities. A realistic lower limit for R_0 results from the increasing difficulty of producing the corrugation of the theta-pinch plasma necessary for equilibrium.

3. We may abandon the condition of a closed configuration and investigate only a torus segment. As a limiting case (i. e. in approaching a straight section) this alternative also includes the corrugated linear theta-pinch LIMPUS, where the stability can be considered independent of the equilibrium problem. However, the question now arises as to whether the experimental results obtained with open ended configurations can be meaningfully applied to closed geometries. The presence of the ends might influence the stability condition through the changed velocity distributions, by additional regions of favourable magnetic field curvature outside the coils, or by "line tying". Pressure perturbations from the ends propagate at approximately the ALFVEN velocity v_A along the plasma column [21], so that for a sufficiently long coil there is a usefully long observation time for the undisturbed plasma far from the ends.

M & S experiments on a toroidal theta-pinch have been caried out for the following parameters: $R_0 = 26$ cm; $r_0 = 3.5$ cm; $T = 5 - 10$ eV; $B_{max} = 11$ kG. These parameters thus correspond to the conditions covered in points 1 and 2.

The rapid diffusion which is characteristic of this case, and the corresponding short lifetime of the high β state in which we are interested, are compensated by the fact that in a torus of smaller radius other characteristic time scales are also shortened, such as the toroidal drift time τ_D in a smooth torus or the instability growth times in an M & S torus.

The experiments described below were carried out during 1964/65 at the Max-Planck-Institut at Munich extending earlier experiments reported elsewhere [60–63]. The only relevant theoretical treatment available at that time was the paper by MEYER and SCMIDT [28].

In the absence of theoretical guidance for shaping the magnetic field of an M & S configuration, our experiments were primarily concerned with investigating the effect of various M & S-like corrugated magnetic field geometries on the behaviour of the plasma. The experiments can be divided into two

[60] W. LOTZ, E. REMY, and G. H. WOLF, Nucl. Fusion **4**, 335 [1964].
[61] U. GROSSMANN-DOERTH, W. LOTZ, E. REMY, and G. H. WOLF, Phys. Rev. Lett. **10**, 1, 5 [1963].
[62] W. LOTZ, F. RAU, E. REMY, and G. H. WOLF, ESPP, Eurat, Symp. Plasma Phys., Varenna, Brussel, Informations Nr. 15 763 e, f, Part III [1964].
[63] W. LOTZ and E. REMY, Max-Plack-Institut für Physik und Astrophysik, München, Report MPI-PA-6/62 [1962].

groups which differ according to the method of producing the magnetic fields. In the first method [61], separate auxiliary coils were used to superimpose a corrugation upon a purely azimuthal (B_φ) main field. In the second method, the inner surface of the main coils was shaped so that they themselves produced a net corrugated field.

For method one: a glass torus of circular cross section was fitted with windings to produce a (purely azimuthal) B_φ field. The auxiliary windings to produce the magnetic field corrugation were mounted on the inner side of the torus (i. e. near the major axis) and supplied with variable currents. The windings for the B_φ field consisted of two concentric solenoids through which currents flowed in opposite directions to produce zero net azimuthal current.

Fig. 9 * shows a torus section at the position where current is supplied to the B_φ winding from a collector. The 31 μf capacitor bank was charged to 16 kV and produced a maximum B_φ field of 11 kG with a ringing frequency of 30 kHz. A pre-ionization bank connected to the same collector and charged to 25 kV produced a maximum B_φ field of 2 kG at a frequency of 200 kHz. The dimensions of the torus were: $R_0 = 26$ cm (major radius of torus); $r_s = 3.8$ cm (inner coil radius); and $r_g = 3$ cm (inner radius of glass vessel). The auxiliary windings were first mounted as shown on Fig. 9 (b). The auxiliary current (in the $z = 0$ plane) flowed alternatively in the direction of the current producing the main B_φ field, which is locally increased, and in the opposite direction, to decrease the main field. The number of these periods around the major torus circumference was varied and 16 periods were found to give the best results. During these early experiments [63] it was not realized that the auxiliary current leads should have passed through the glass vesel to produce the desired magnetic field configuration. Later this problem was recognized and the auxiliary windings were passed through the glass vessel by means of glass tubes or notches. In this way the acceleration, b_R, of the plasma (the toroidal drift arising in purely azimuthal fields) was eliminated by a suitable adjustment of the current in the auxiliary windings [61]. In addition to providing the correct current magnitude, it was also necessary to switch on the main and auxiliary fields simultaneously.

A new effect now appeared, however, consisting of a compression of the plasma column towards the $z = 0$ plane and a simultaneous spreading out in this plane. This spread was caused by too small a corrugation of the magnetic field perpendicular to the $z = 0$ plane, which made the magnetic pressure perpendicular to this plane larger than that along the outer and inner contour of the plasma surface (in the $z = 0$ plane). This means that the δ_2 component, from Eq. (19), of the applied magnetic field was not adjusted correctly. To overcome this problem a new arrangement of auxiliary windings was used in which the currents flowed not only along the inner side of the torus but along the top and bottom as well. A section of such a torus — whose appearance gave rise to the name "crown torus" — is shown in Fig. 10 **. The results obtained with the "crown" torus can be summarized as follows:

(a) The plasma behaviour was not adequately reproducible either in time or space, i. e. from period to period around the torus circumference. The reason was presumably that the mechanical mountings for the auxiliary windings were not sufficiently accurate and rigid. The confinement time could be extended up to a factor of 3 above the same discharge without current in the auxiliary windings; in the latter case (i. e. without auxiliary current) the toroidal drift time τ_D was observed to be the same as in a smooth vessel (circular cross section) without any additional windings.

(b) The shape of the auxiliary windings could be varied as shown in Fig. 11, to produce plasma spreading in the $z = 0$ plane (δ_2 too small), as already discussed or, in the other extreme, perpendicular to the $z = 0$ plane (δ_2 too large). The times shown in Fig. 11 correspond to ~ 3 μsec.

All efforts to find an intermediate position of the auxiliary windings between these two extremes, such that all spreading was completely avoided and the plasma column remained in the centre of the tube, however, were unsuccessful. Although for the first $2-3$ μsec the plasma column maintained a circular cross section with the best winding arrangement used (for the two extreme positions some spreading could already be distinctly observed during this time), nevertheless a spreading or net displacement of the plasma always occured at later times. Further experiments were therefore required to determine

* Fig. 9 on page 1002 b.

** Fig. 10—13 on page 1012 a.

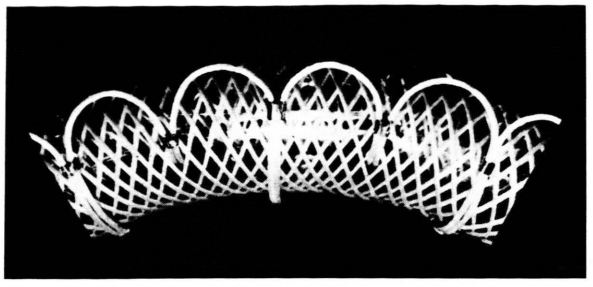

Fig. 10. Section of "crown torus" on which the B_φ windings as well as the auxiliary "crown-like" windings are visible [60].

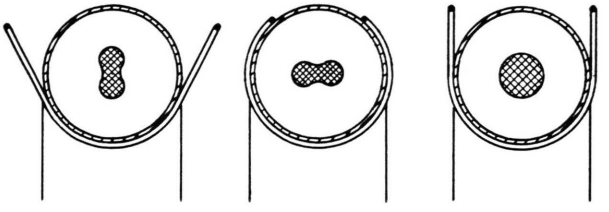

Fig. 11. Influence of different arrangements of the auxiliary windings used on the "crown torus", shown schematically in a $\varphi = \text{const}$ plane.

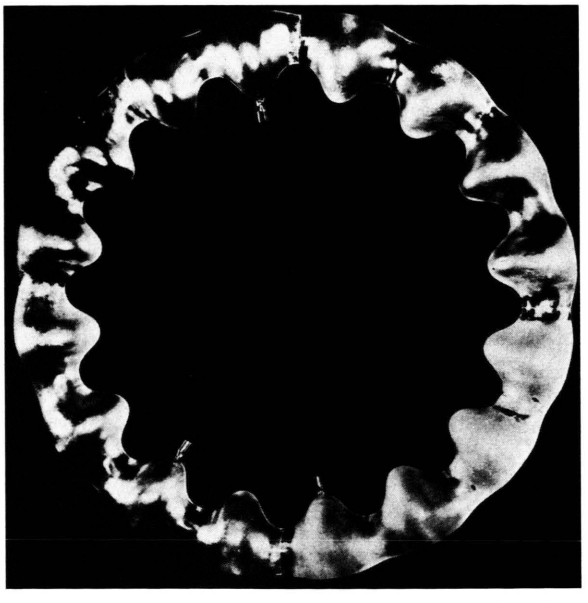

Fig. 12. Photograph of pyrex glass discharge vessel based on the M & S surface (above) of Fig. 3.

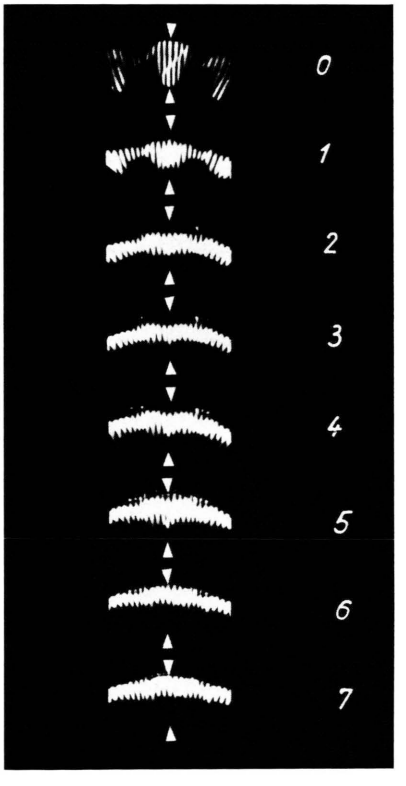

Fig. 13. Image converter photographs taken with visible light from successive discharges (40 mtorr H_2, at $B_{max}=11$ kG, with pre-ionization) in vessel of shape 1 with equidistant loops [62]. The times when exposing are given in μsecs; the exposure time was 0.3 μsec. ⟶

whether the end of the confinement was due to inaccuracy in placement of the windings or to instabilities.

For method two: use was made of the fact that suitable magnetic field configurations can also be obtained by proper shaping of the coils themselves. The inner surface of a theta-pinch coil represents a magnetic flux tube for the time period of interest, because of the skin effect.

Since the strong forces which are exerted on a coil structure by the large magnetic fields are in part responsible for the problems discussed above under method one, the method of coil shaping represents a technically easier way of producing the desired M & S fields. Additional windings can be provided in the coil interiors to produce small corrective fields of variable amplitude and phase.

For the production and confinement of an M & S plasma by means of this technique, three requirements should be satisfied:

1. After the fast theta-pinch compression the plasma surface must take on M & S geometry.

2. The strength of the confining magentic field must simultaneously fulfil the conditions for equilibrium.

3. Finally, during the adiabatic compression phase of the discharge, the field configuration must change in acordance with the changing volume of the plasma column.

Apart from the programmed corrective field mentioned above, two independent parameters (within limits) are availabe for satisfying these three requirements:

(a) The shape of the inner coil surfaces;

(b) The shape of the discharge vessel, which then determines the initial mass distribution and the flux tube tangent to the plasma surface.

In the case of the experiments described below, no calculations were available for either the confining magnetic field which determines the coil shape or for the dynamics of the fast compression from which the vessel shape has to be determined. The experimental problem thus consisted of empirically testing various vessel and coil shapes. Because of the multitude of possible 3-dimensional shapes, the search was limited to an examination of the tendencies in the plasma behaviour as affected by different shapes. Two different vessel shapes were tested in conjunction with several coil shapes and no additional auxiliary windings were used.

The first vessel shape (shape 1) was based on a numerically calculated $\beta = 1$ M & S surface, with 16 periods around the major torus circumferences and with approximately the same volume as the equivalent smooth torus. The diameter at a "bulge" was 9 cm. The selected shape is shown in Fig. 3 above and a photograph of the pyrex glass discharge vessel is shown in Fig. 12.

The first type of coil spanned each M & S period with 12 equi-distant copper loops (this spacing in accordance with the simple M & S picture), electrically connected in parallel.

With this arrangement the plasma column remained at the centre of the vessel for $2-3$ μsec following the fast theta-pinch compression, and then drifted towards the vessel wall in $+R$ direction, reaching the wall about 6 μsec after the start of the compression. The confinement time was thus increased by a factor $3-4$ compared with an equivalent discharge in a purely azimuthal magnetic field (i. e. with the toroidal drift time τ_D).

The behaviour of the plasma can be seen in Fig. 13, which shows a series of image convertor photographs of successive discharges in hydrogen at 40 mtorr, taken at 1 μsec intervals looking perpendicularly to the $z=0$ plane. The inner vessel wall is indicated by the apexes of the white triangles.

In addition Fig. 13 shows that immediately following the fast compression the plasma surface has an M & S-like shape which, however, increasingly smooths itself out during the next few microseconds so that this initial corrugation nearly disappears during the above mentioned drift phase.

Simultaneous photographs were taken at 90° from above, sighting along the major radius R in the $z=0$ plane, to furnish a stereoscopic picture. These showed that the plasma tended to spread out perpendicularly to the $z=0$ plane during its drift to the wall.

When compared with results from the "crown torus", the advantages of this new technique (i. e. with shaped vessel and coils) were considered to be not so much the slightly increased confinement time as the high reproducibility of the individual discharges as determined from image converter photographs and spectroscopic measurements. Thus it was possible to measure in successive discharges the radial distribution of the H_β line and the continuum radiation (4200 Å) by scanning from the centre to the edge at the "necks" and "bulges" of the corru-

gation and from these measurements to deduce temperature and density distributions [65]. The resulting temperatures are compared in Fig. 14 to the temperature obtained in the equivalent smooth (purely azimuthal field) theta-pinch.

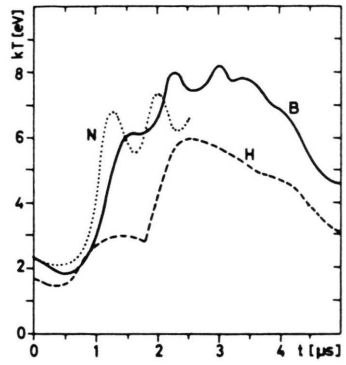

Fig. 14. (a) Time variation of T_e at the "necks" (H) and "bulges" (B) of a shape 1 type discharge (40 mtorr H_2, at $B_{max}=11$ kG with pre-ionization and equi-spaced loops) and in the corresponding smooth torus (N).

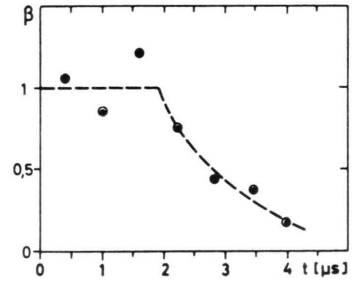

Fig. 14. (b) Time dependence of β_{max} (on the axis of the plasma column) at the bulge in the same shape 1 discharge (relative error $\sim 20\%$).

It can be seen that the "bulge" temperatures agree closely with those from the corresponding smooth torus (during the drift time). The same figure also shows the time dependence of β_{max} existing locally on the axis of the plasma column. As a next step, various non-equidistant loop arrangements were used in order to investigate other magnetic field geometries. Typical results of these experiments are shown in Fig. 15, which are image convertor photographs taken at 2 and 3 μsec. The top photographs show discharges in the equidistant loop arrangement corresponding to Fig. 14. The second row of Fig. 15 shows discharges for which the current loops are pinched together at the necks to increase the corrugation of the magentic field. Accordingly the position of the plasma column is displaced towards the major torus axis $R=0$ to such an extent that possible contact with the wall at the inner side of the necks could not be discounted. This is even more evident in the next two pictures in row three, where the plasma touches the wall along most of the inner vesel contour; thus, because of the closer spacing of the loops, the corrugation of the magnetic field was such that the initial drift motion was reversed.

The parallel-connected copper loops which were used as field coils in these experiments had two disadvantages. Firstly, it was found that in the "neck" regions some of the magnetic flux passed outside the tube formed by the loops so that the intended shape of the flux tubes was not completely achieved. Secondly, currents were necessarily constrained to the loops and could not flow axially. To overcome both these disadvantages, in the following experiments the field coils were formed of massive shells, pressed from 1.5 mm thick copper sheet, which surrounded the glass vessel with a gap of 1 mm and which at the discharge frequency of 30 kHz were not penetrated by the magnetic field lines. To enhance or weaken the corrugation, variously shaped wedge-like sections were cut from the coil bodies at the neck regions as shown schematically in Fig. 16. The plasma behaviour was investigated at initial pressures of 10, 20 and 40 mtorr and the figure shows four characteristic sequences of image converter photographs (at 40 mtorr) in which tendencies similar to those in Fig. 15 with variably spaced loops can again be detected. Whereas in sequences 1 and 2 the original outward drift was over-compensated because of the too strongly corrugated inner contour of the magnetic field, 4 μsec after initiation of the discharge in sequence 4 an outward drift is observed similar to the plasma behaviour in Fig. 14. In sequence 3, on the other hand, the centre of gravity of the plasma remains nearly unchanged after 4 μsec but the plasma column begins to spread out as in sequence 1 and 2. This spreading or fanning tendency becomes even more evident in discharges at 10 mtorr. An example is shown in Fig. 17, taken at $t=8$ μsec with the same sheet coil arrangement used in sequence 3 of Fig. 16. That photograph also shows that the plasma column eventually splits into several filaments. The actual confinement time for 10 mtorr discharges was only $3-4$ μsec, however, since by this time there was usually contact between the plasma and the walls.

[65] These measurements were carried out together with J. JUNKER.

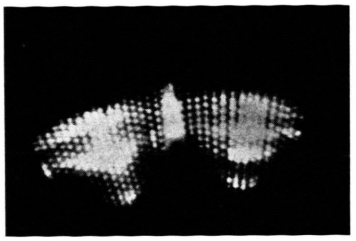

Fig. 17. Image converter photograph at $t=8\,\mu$sec (10 mtorr H_2, $B_{max}=11$ kG, with pre-ionization). The arrangement of the field coils is the same as in sequence 3 of Fig. 16. This photograph shows the splitting of the plasma column into at least three separate filaments, suggesting an $m=4$ instability.

Fig. 15. Image converter pictures of shape 1 discharge (40 mtorr H_2, $B_{max}=11$ kG, with pre-ionization) for different current loop arrangements.

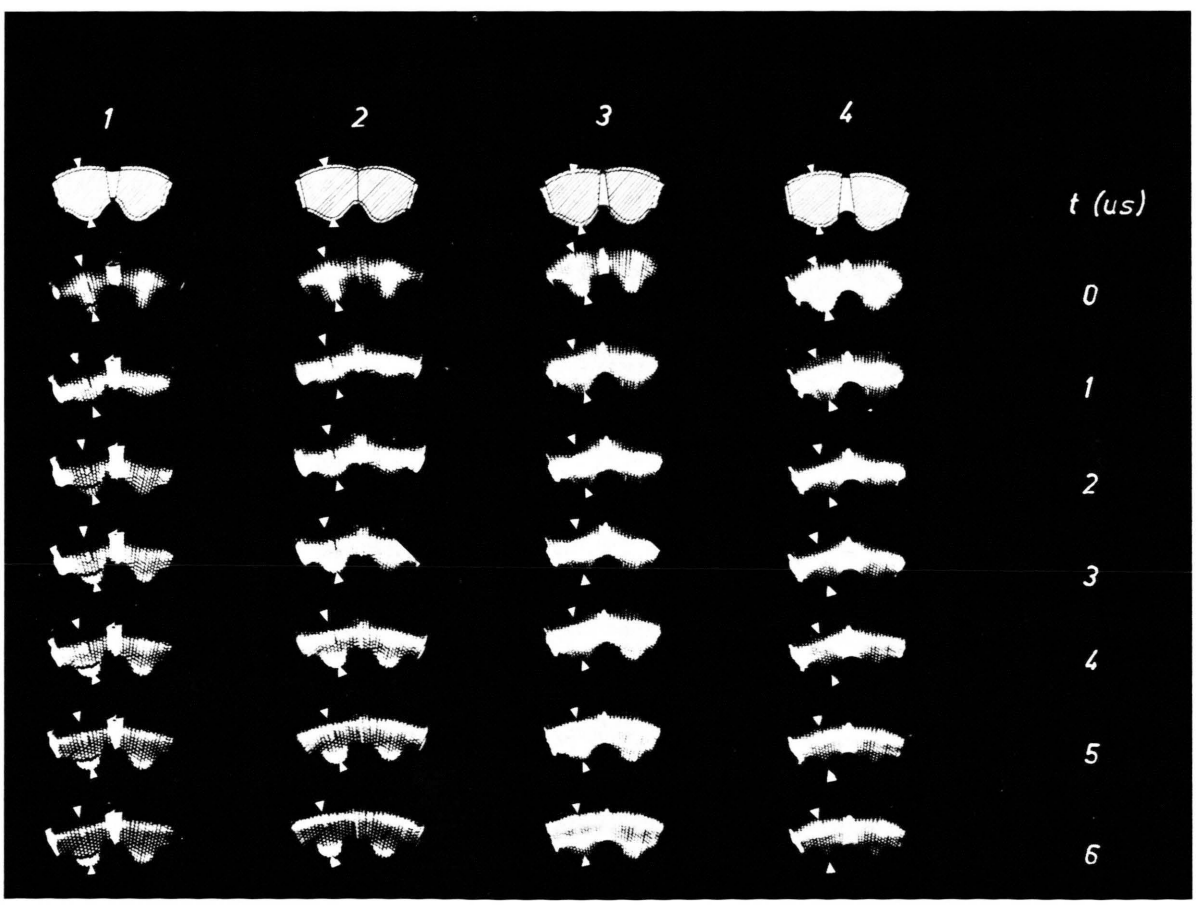

Fig. 16. 4 sequences of image converter photographs of successive discharges (40 mtorr H_2, $B_{max}=11$ kG, with pre-ionization) in type 1 vessels using copper sheet field coils. The white triangles indicate the inner wall of the discharge vessel. The four sequences of photographs are distinguished by different types of sections cut away from the coil body at the neck regions to influence the magnetic field shape.

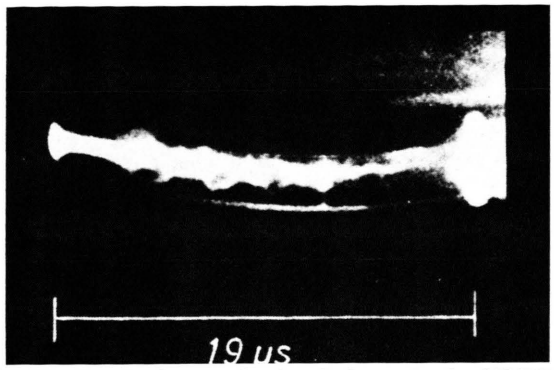

Fig. 19. Streak photograph of a discharge in the LIMPUS coil [50] (observation through slot HB parallel to plane of collector in D_2 at 290 mtorr and a bank energy of 1 MJ). The curvature of the picture is due to the return magnetic flux in the image converter tube and the white fringes outside the plasma column are reflections from the vessel wall. The perpendicular white patch after 19 μsec shows the start of the second half cycle of the main discharge. The (nearly) periodic flares are interpreted as $m > 2$ instabilities.

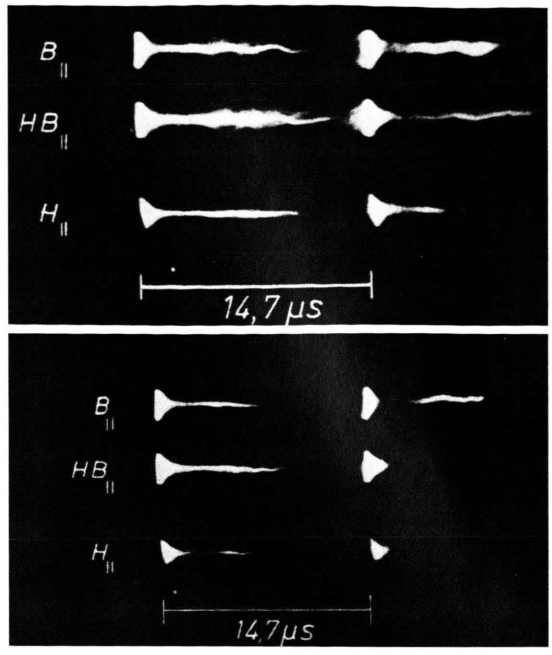

Fig. 20. Streak photographs of discharge with the LIMPUS coil [50] (direction of observation parallel to the collector slot) for a capacitor bank energy of 340 kJ. The bright patch after 14.7 μsec shows the start of the second half cycle of the main discharge. (a) 20 mtorr D_2. Flares are seen through slits B and, especially, HB which are interpreted as $m > 2$ instabilities; (b) 10 mtorr D_2. No flares are visible.

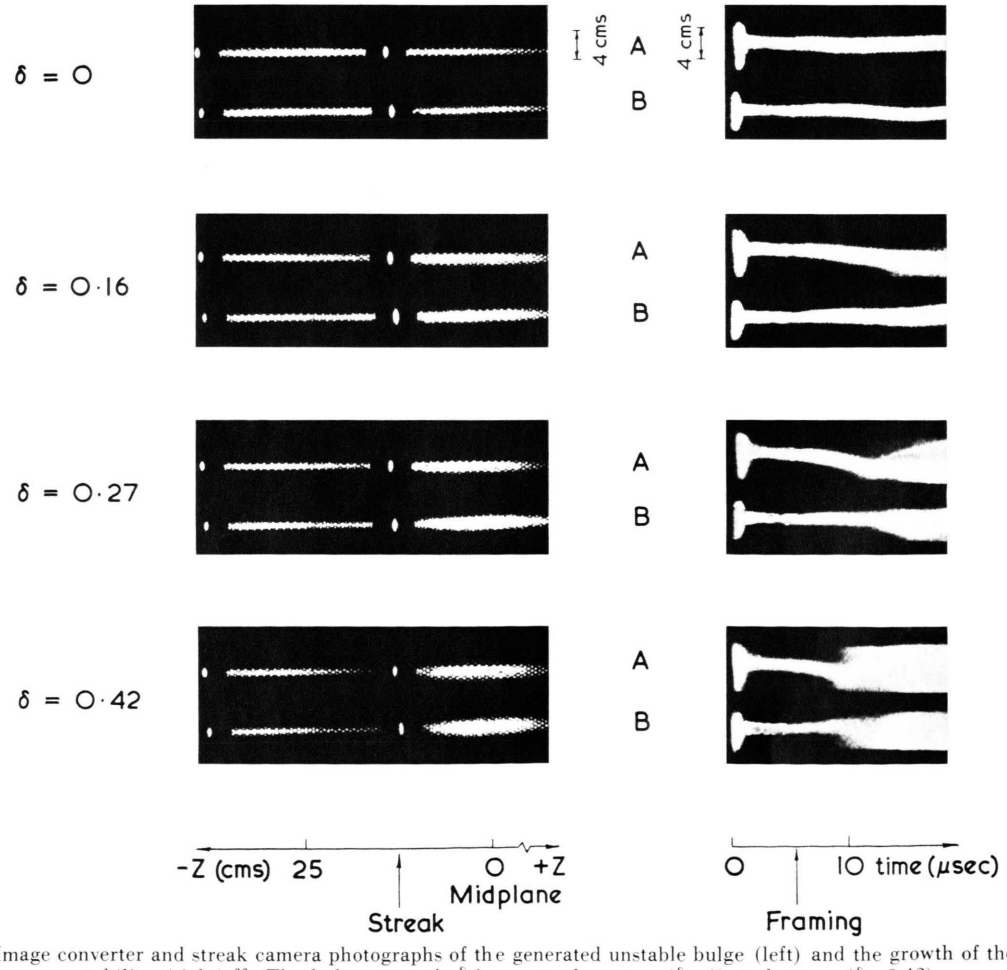

Fig. 23. Image converter and streak camera photographs of the generated unstable bulge (left) and the growth of the $m=1$ instability (right) [66]. The bulge strength δ increases from top ($\delta=0$) to bottom ($\delta=0.42$).

In the final series of experiments, a second discharge vessel (shape 2) was used in which the overall corrugation was shallower than in shape 1.

The surface of this vessel was formed from a calculated M & S surface for a thinner plasma column (shown in Fig. 3 below) by adding to this shallower corrugation a constant 2 cm radius to produce a surface of the same average diameter as shape 1. As before, coils with various corrugation amplitudes were used.

The behaviour of the plasma in shape 2 was qualitatively similar to that shown in Fig. 14, although the time during which the plasma remained in its centrtal position was so brief and uncertain that the plasma column had already reached the vessel wall in 3 – 4 μsec. It is concluded that shape 2 was a poorer approximation to the equilibrium condition than shape 1.

The M & S experiments described here can be summarised and interpreted as follows:

1. The acceleration of the plasma centre of gravity (the "toroidal drift" in a purely azimuthal magnetic field) could be either reduced, reversed or eliminated. In the latter case the geometry of the plasma surface initially agreed, qualitatively, with an M & S surface. By comparison with the equivalent smooth torus, the confinement time was increased by a factor of about 3 – 4, for a plasma of about the same temperature and density.

2. The plasma column at first remained in the centre of the tube for several microseconds while the initially corrugated shape gradually smoothed out. Subsequently, an outward drift of the entire plasma column was observed. The smoothing process which was due to the decrease of β with time as a result of classical diffusion, modified the configuration originally set up for providing equilibrium. For this reason it could not be stated whether or not the observed drift was caused by an $m = 1$ instability.

3. In some series of experiments flute instabilities of the type $m \geqq 2$ developed towards the end of the confinement time, in accordance with the MHD-model [Eq. (44)], and these instabilities competed with the processes mentioned above to limit the plasma confinement.

4. However, the obvious agreement of the observed confinement time with a calculation based on the MHD instability [Eq. (54)] suggests, firstly, that the low-m MHD modes play a substantial role in limiting the confinement time and, secondly, that the configuration originally set up represents an adequate approximation to the equilibrium required. Thus these experiments have answered the question we posed in the affirmative.

To gain experimental evidence about the remaining uncertainties concerning, in particular, the stability characteristics of an M & S configuration, linear theta-pinch experiments in MHD-unstable configurations have been carried out where, on the one hand, the pressure profiles and the value of β remained sufficiently constant during the observation time and where, on the other hand, it is less difficult to distinguish between the equilibrium and stability problems.

5. Linear Stability Experiments

In the case of MHD unstable linear theta pinch configurations, e. g. in the corrugated LIMPUS geometry (Fig. 7), the toroidal problems were replaced by end-effect problems. End signals propagate along the plasma column not faster than with about the Alfven velocity, v_A. Thus, in order to obtain a sufficient time for stability observations without end influences, one requires coils about 10 m long. In view of the capacitor banks available at present this means that the attainable magnetic fields are not sufficient to heat and confine collisionless theta-pinch plasmas. Pending the completion of the Scyllac bank [17] one thus has the choice of either investigating collisionsless plasmas in coils which are too short, or collision-dminated plasmas in sufficiently long coils. In both of these regimes stability experiments have already been carried out [21, 55, 66].

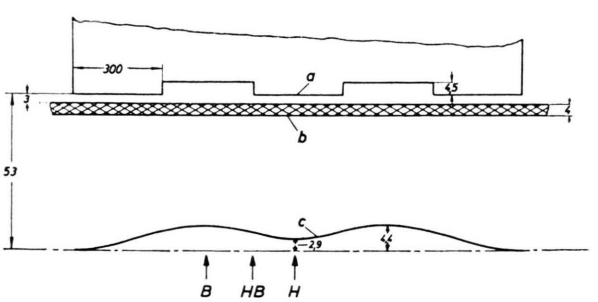

Fig. 18. LIMPUS geometry. *a*, coil surface; *b*, vessel; *c*, plasma; (in mm). *r* scale = 1 : 1, *z* scale = 1 : 10. B, HB, and H are positions of observation slits [50].

[66] H. A. B. Bodin, A. A. Newton, J. Wesson, and G. H. Wolf, submitted for publication to Phys. Fluids [1968].

In the preliminary LIMPUS experiment in Munich using the "Isar I" bank [50, 56], the normal theta-pinch coil of 150 cm length was subdivided into five sections having different diameters (Fig. 18), so that even the fast compression of the plasma took place in a corrugated configuration. The experiments utilized Z-pinch pre-ionization, and the capacitor bank energy was either 340 kJ or 1 MJ (peak magnetic field of 110 kG in 10 μsec); the results were insensitive to the different capacitor energies used. The gas was D_2 at an initial pressure of 10 mtorr or 20 mtorr. The maximum electron densities reached were in the region $n_e = 2 \cdot 10^{16}$ cm^{-3} (from the centre-edge distribution of the continuum radiation) and the maximum of kT_i was in the region of 3 keV (from the neutron yield).

With the normal (smooth) linear theta-pinch coil [6], the plasma column moved from the coil axis to an excentric position in direction of the collector slit during an $8-9$ μsec period from the end of the fast compression. The maximum deviation was about 3 cm. The reason for this displacement was an asymmetry of the magnetic field arising from the particular collector arrangement used. The plasma column executed additional oscillatory or pendulum-like movements in the direction which correspond to the "wobbling" motion also observed elsewhere [18], and which may partly be due to a rotation of the entire plasma column.

The corrugated magnetic field produced by the shaped LIMPUS coils did not affect either the extent of the plasma displacement or its subsequent wobbling motion. However, the time required for the plasma column to reach its displaced position was shorter than when using the normal coil. This more rapid displacement allows two conflicting interpretations:

1. faster attainment of an excentric equilibrium, which suggests improved $m = 1$ stability or,

2. faster growth of an $m = 1$ instability already present in the uncorrugated case. A choice between these two is complicated by the fact that end-effects became involved on this time scale.

The periodicity in the wobbling motion has been correlated to the appearance of flares emerging from the sides of the plasma column as shown in Fig. 19. This phenomenon occurred at 20 mtorr but not 10 mtorr, and was interpreted as an $m \geqq 2$ instability. The absence of $m \geqq 2$ instabilities at 10 mtorr in the streak photographs was confirmed independently from the time variation of the measured line density, from the total neutron yield, and from the time variation of the neutron flux. None of the above measurements showed significant differences between discharges with corrugated and normal uncorrugated coils. Fig. 20 shows streak photographs of "corrugated" discharges taken at (a) 20 mtorr and (b) 10 mtorr through the observation slits $H_{||}$, $HB_{||}$ and $B_{||}$ ($||$ means viewing parallel to collector slot). It is worth noting that the flares which occur at 20 mtorr are most prominent through the slit $HB_{||}$.

In addition to the obviously different dynamic processes between discharges at 10 and 20 mtorr, there is the important difference that in the 10 mtorr discharges most of the neutron yield is produced during the first half cycle of the main discharge, whereas at 20 mtorr a measurable neutron flux occurs only during the second half cycle. Since the first half cycle is the one of interest, the 10 mtorr plasma is thus in an entirely different regime ($kT_i \approx 3-4$ keV) from the 20 mtorr plasma.

Measurements of the centre-edge distribution of continuum radiation were made through the slits $H_{||}$ and $B_{||}$, and the corresponding density profiles were determined. This yields the pressure profile on the

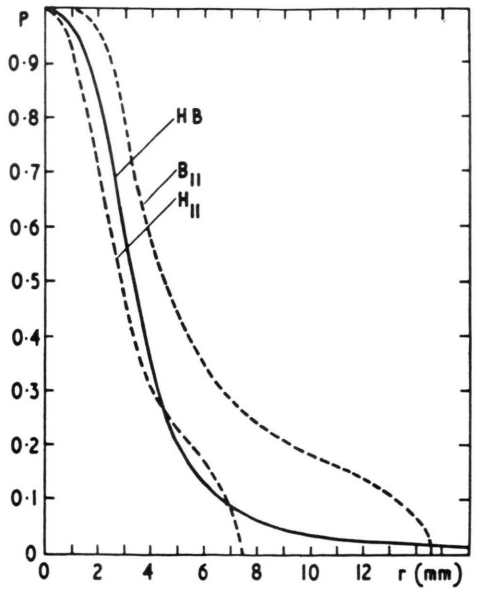

Fig. 21. Radial pressure profiles (normalised) of a LIMPUS plasma [50]. The dashed lines H and B represent density profiles (which correspond to pressure profiles) determined from continuum measurements 8 μsec after initiation of a 10 mtorr D_2 discharge. The solid line HB is used for calculating [37] the field configuration shown in Fig. 5.

assumption that temperature is position independent. In Fig. 21 the dashed lines H and B indicate the pressure profiles, at the neck and bulge respectively, which were found for 10 mtorr discharges 8 μsec after initiation of the discharge, p_{max} being normalized to 1. The plasma neck and bulge radii, corresponding to p_{max}, together with a mathematical approximation to the pressure profile (solid line HB) were used as a basis for the calculation [37] which yielded the magnetic field configurations of Fig. 5. The corrugation amplitude of the calculated magnetic field in the region of the coil agrees well with the corresponding size of the coil instep, shown by the dashed line in Fig. 5. The near-sinusoidal shape of these outer field lines, does not, however, agree with the stepped coil shape.

One must conclude, therefore, that the plasma surface $r_p(z)$ acquires a more rectangular axial variation than the smooth shape shown. To obtain some further information about the axial shape the plasma surface for a given stepped coil form was calculated for the special cases of $\beta = 0$, and $\beta = 1$ with surface currents [67]. From this one can estimate a reduced period length L', for which, whilst retaining the corrugation amplitude, a sinusoidally shaped surface is obtained with the same $\int (dr_p/dz)^2\, dz$ as the actual LIMPUS configuration of period length L. L' is estimated to be between 20 and 40 cm; for $L' = 30$ cm and $kT_i = 3$ keV, Fig. 8 shows the calculated MHD growth times where (from Fig. 20) the value of δ is roughly between 0.2 and 0.3.

The Alfvén transit time from the open ends to the mid-plane of the coil is approximately $2-4$ μsec (in the high pressure regions), whereas the predicted MHD growth times are less than one microsecond. The fact that at 10 mtorr no $m \geqq 2$ instabilities have yet been observed lends support to the assumption that some damping process becomes effective to suppress these $m \geqq 2$ flutes in collisionless slim high β plasmas.

In order to eliminate end effects for a sufficiently long time and thus to permit study of some still open questions, especially concerning the MHD $m = 1$ mode, a stability experiment was carried out at CULHAM [21, 66] using the Megajoule bank to drive an 8 m linear theta pinch. The peak magnetic field of 21 kG was reached after 5.5 μsecs (crowbar decay time 160 μsecs), producing a collision-dominated plasma with a peak electron density of 3×10^{16} per cm^3 (filling pressure 20 mtorr D_2) and a temperature of about 120 eV. The plasma radius was ~ 1 cm.

Instead of a periodically corrugated LIMPUS-type configuration, only a single bulge (in the mid-plane of the coil) was produced; and in contrast to the Garching LIMPUS experiment the inhomogeneity of the magnetic field was set up after the fast compression had been completed and mass oscillations had damped out [68]. The stability properties of such a single-bulged configuration, however, are not expected to differ substantially from a similar periodic corrugation [71]. In order to compare the experimental growth rates with the square profile calculations leading to Eq. (47a), an average value $\langle\beta\rangle \approx 0.4$ (estimated by independent methods [66]), has been used instead of the peak value of $\beta_0 \approx 0.7$ on the axis of the plasma column. In addition $\langle\beta\rangle$ is used to evaluate $\langle v_A\rangle$ by the relation

$$\langle v_A\rangle = v_{A0}\sqrt{\beta_0/\langle\beta\rangle}.$$

The method for generating the unstable bulge is shown schematically in Fig. 22. One 25 cm long section of the coil is crowbarred a time interval Δt before it would have reached peak field, the time

[67] F. HERTWECK, Eurat. Symp. Theor. Plasma Phys., Part I, 89 [1966].

[68] It is doubtful whether in a toroidal M & S experiment the corrugation can also be produced only after completion of the fast compression. The experiences accumulating during M & S experiments with additional currents, during the "Spinne" experiment [69] and with the screw pinch [70] have shown that the time relation between main field and additional field is important in preventing the toroidal drift.

[69] G. v. GIERKE, W. LOTZ, F. RAU, E. REMY, and G. H. WOLF, Max-Planck-Institut für Physik und Astrophysik, München, Report MPI-PAE/Pl. 4/65 [1965] und G. v. GIERKE, F. W. HOFMANN, W. LOTZ, F. RAU, E. REMY, H. WOBIG, and G. H. WOLF, PPCNFR CN-21/51, Culham 1965. — Institut für Plasmaphysik, Report IPP 1/44 [1966].

[70] C. BOBELDIJK, L. H. TH. TIETJENS, P. C. T. VAN DER LAAN, and F. TH. DE BATS, Plasma Phys. **9**, 13 [1967].

[71] In analogy to Eq. (47) — square pressure profile — the MHD growth time of the $m=1$ mode (for small δ) is

$$\tau_{m=1} = \frac{L(2-\beta)^{3/2}}{2\pi^2 v_A \delta'^2 \beta(1-\beta)(3-2\beta)} \qquad (47\,a)$$

where v_A is again $B_a^*\sqrt{4\pi\varrho}$ (ϱ density in the unperturbed plasma), but $\delta' = \delta/1-\delta$ when considering one period of Fig. 7 as a single bulge. For large δ' the axial coupling between the bulged region and the rest of the plasma column is reduced; then the δ'^2 scaling of Eq. (47 a) gradually changes to a δ' scaling similar to Eq. (47), according to numerical calculations [66].

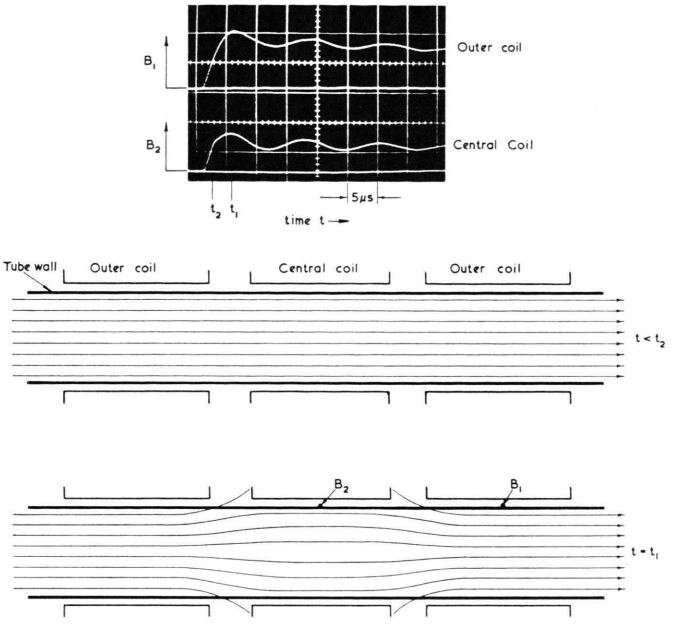

Fig. 22. Schematic diagrams showing method used for generating the unstable bulge [66]. The oscilloscope photograph shows the current traces for the field shaping coil and for the neighbouring coil, being crowbarred at different times.

at which the other coil sections are crowbarred. The magnetic field in the coil which is crowbarred early, known as the field shaping coil, rises more slowly than the magnetic field elsewhere and so a bulge develops; plasma flows from the regions on either side into the bulge. The amplitude of the bulge and thus the value of δ for a given magnetic field ratio B_1/B_2 depends on $\langle\beta\rangle$. Due to the effect of the slot the magnetic field configuration in the region of the bulge is not completely symmetrical with respect to the axis of the coil; any asymmetry can lead to a lack of equilibrium of the plasma in the unstable region, from which a drift of the column results. To study the non-axisymmetric field components three-dimensional field plots were obtained throughout the volume of the field shaping coil (on a model bank). It was found that for the coil spacing used the asymetrical field curvature was approximately 1% of the symmetrical component of the curvature (in the direction of the slot), which was estimated as to weak to cause the plasma motion observed, this in particular, since the axial average of this curvature is essentially zero.

Fig. 23 shows a series of stereoscopic streak and framing camera photographs taken in the neighbourhood of the unstable bulge. The directions of observation (A) and (B) correspond to viewing the plasma 45° above and below the horizontal. Four pairs of photographs are shown corresponding to different bulge strengths; from top to bottom, δ increases from 0 to 0.42. The framing camera photographs, which include the field shaping coil (right) and neighbouring coil (left) were taken through perforated coil sections (1 μsec exposure time) 6 μsec after the start of the discharge. The formation of the unstable bulge can be seen by comparing the plasma diameter in the shaped region to that in the unshaped region; it should be noted that in particular for strong bulges (e. g. $\delta = 0.42$) there is a marked reduction in the intensity of the light coming from the end of the shaped region. This is due to an $m = 0$ rarefaction wave moving outwards from the shaped regions along the column, as plasma flows from neighbouring coil sections to fill the bulge. The streak camera photographs on the right hand side of Fig. 23 were taken in the slot between the shaped and unshaped coils (ω independent of z!). The top photograph shows the low amplitude lateral motion present in the discharge column with no field shaping. The growth of the $m = 1$ instability for $\delta = 0.16$ up to $\delta = 0.42$ can be seen on the streak photographs. The instability grows more rapidly with increasing δ from top to bottom of this figure and the time at which the plasma strikes the wall as a result of the instability is seen to decrease with increasing bulge strength.

The data in Fig. 23 were analysed to yield values of the amplitude of the instability, $\xi(t)$, as a func-

tion of time. $\xi(t)$ is defined as the displacement of the plasma axis from its average initial position before the instability started to grow. Values of $\xi(t)$ are plotted in Fig. 24 for different bulge strengths δ

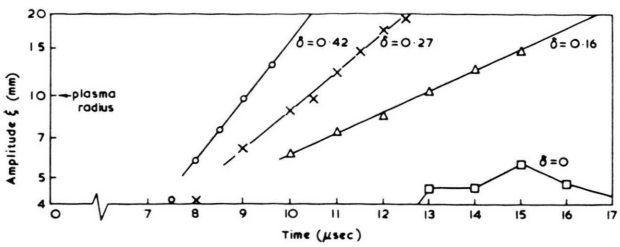

Fig. 24. The amplitude $\xi(t)$ of the observed $m=1$ instability as a function of different bulge strengths δ. ξ is plotted on a log scale [66].

on a log scale, and it is seen that during the linear phase of the instability, when its amplitude is comparable with the plasma radius, the points lie on a straight line indicating an exponential growth. The slope of the line varies with the bulge strength δ; the strongest bulges have the largest slopes, corresponding to the fastest growth rates. The equivalent ξ for a discharge with no field shaping is also plotted; the data for $\delta>0$ were not corrected for this motion, which set a lower limit for measurable growth rates. Below $\delta=0.1$ the $m=1$ instability no longer hit the tube wall but was damped or even reflected in the neighbourhood of the wall. In such cases a rotating $m=2$ perturbation was observed to develop, similar to that occurring at later times, when influences from the ends, propagating axially with Alfvén velocity, could reach the mid plane.

Values of the growth rate $\omega=1/\tau$ for the $m=1$ instability were obtained from the slope of the lines in Fig. 24, and are plotted in Fig. 25 as a function of the bulge strength δ. Each experimental point in this figure represents one discharge, so that the spread between the different points gives a measure for the reproducibility.

Fig. 25 also shows the theoretically computed growth rate as a function of δ [for small δ according to Eq. (47a)] assuming two different period lengths L of the unstable region.

There is some uncertainty about the experimentally achieved length L of the bulged regions. The length of the field shaping coil was 25 cm, and vacuum field measurements made with this coil on a model bank indicate that L may be somewhat grea-

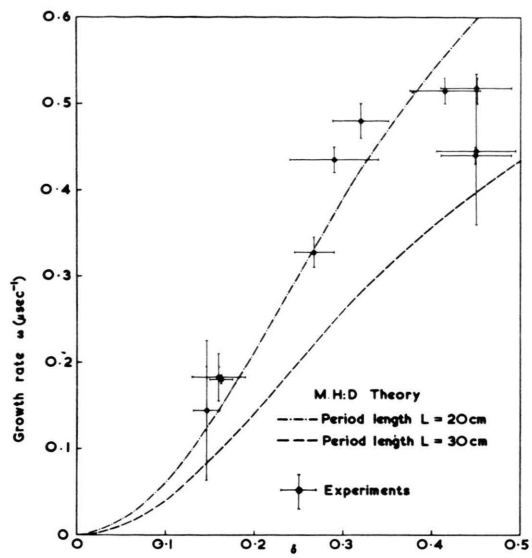

Fig. 25. The growth rate $\omega=1/\tau$ of the $m=1$ instability as a function of bulge strength δ [66]. The experimental points are taken from the slope of log $\xi(t)$ (Fig. 24). The theoretical curves are computed from ideal MHD theory for $\langle v_A\rangle=2.4\times10^7$ cm/sec.

ter than the coil length. On the other hand the streak and framing photographs indicate that the value of L of the bulged plasma column might be even somewhat smaller than this length, which is believed to be a consequence of the axial dynamics, i. e. the $m=0$ rarefaction wave. Thus for the plots of the theoretical results $L=20$ cm was used as an estimated lower limit, and $L=30$ as an estimated upper limit.

The experimental points in Fig. 25 are obviously in good agreement with the theoretical curves, although the differences between the theoretical model (square pressure profile, axial equilibrium) and the experimental plasma configuration (smooth pressure profile, axial reaction wave), which made it necessary, for instance, to introduce the averages $\langle\beta\rangle$ and $\langle v_A\rangle$, could potentially account for discrepancies of perhaps up to a factor of two.

For diffuse pressure profiles, according to the MHD-model, the growth times for the $m>2$ modes are about the same as for the $m=1$ mode. Since during the available observation time, viz. at least three $m=1$ growth times before the plasma hit the wall, no higher modes were detected, their growth rates are apparently damped by a factor of at least three, an effect which is attributed to finite Larmor radius stabilisation [Eq. (52)]. The experiment

shows, however, that the growth of the $m=1$ instability is well described by the ideal MHD model. Since this instability is unlikely to be sensitive to the detailed pressure profile, the particle mean free path, or to Larmor radius effects – because the driving force is acting on the plasma as a whole – the results from the MHD model concerning the $m=1$ mode are expected to apply over a wide range of conditions, thus establishing this mode as the most dangerous one for bulged theta pinch plasmas.

6. Conclusion

The M & S configuration gives equilibrium for a toroidal plasma without requiring a net current in the azimuthal direction and without using a rotational transform. Explicit solutions have been obtained thus far only for the two restricted cases $\beta=0$, and $\beta<1$ in the surface current model. The existence of M & S configurations with a continuous radial pressure profile, however, has been proved. The use of the M & S configuration to confine a toroidal theta pinch plasma leads to problems in the establishment of the equilibrium and in particular in its stability.

The difficulties of establishing equilibrium are related chiefly to the dynamic processes taking place during the rapid compression of the theta pinch, and to the proper arangement of the coils which produce the confining magnetic field. However, in experiments with theta pinch plasmas having temperatures near 10 eV the shape of the plasma surface initially agreed, qualitatively, with an M & S surface. During the early stages of the discharge the plasma remained quiescent in the centre of the vessel. The confinement time of the plasma was extended by a factor $3-4$ beyond the toroidal drift time τ_D in an equivalent axially-symmetrical torus. Conclusive evidence about $m=1$ MHD stabilities was masked by the decrease of β with time due to classical diffusion.

The stability of the M & S configuration was investigated for the simplified case of the corrugated linear theta pinch, LIMPUS. For the β values attainable in hot theta pinch plasmas the LIMPUS configuration is theoretically unstable according to the MHD model both with respect to fanning ($m\geqq 2$ flutes) and with respect to a total displacement or kinking ($m=1$). Mechanisms to suppress these instabilities for $m\geqq 2$ are based on finite gyro-radii stabilisation, and for $m=1$, restricted to the case of very high β only, the conducting wall.

In previous LIMPUS experiments, no $m\geqq 2$ instabilities have been observed, although, for a collision-dominated theta pinch plasma free from the influence of ends, $m=1$ instabilities were detected whose growth times agreed with MHD theory. It is not expected that in hot collisionless theta pinch plasmas the growth of these $m=1$ instabilities will be significantly damped, e. g. due to increased viscosity.

An extrapolation of the MHD growth times to a toroidal M & S configuration [Eq. (54)] is in obvious agreement with M & S experimental results. This suggests firstly, that the experimentally produced M & S configurations were an adequate approximation to the required equilibrium and, secondly, that low-m MHD instabilities substantially limited the plasma confinement. However, the above initially quiescent position of the M & S plasma at the centre of the vessel presents a starting point for the application of additional stabilising measures undisturbed by the toroidal drift otherwise (in purely azimuthal fields) already setting in during the fast compression stage.

Dynamic methods were theoretically investigated for stabilising purposes. It was shown on the basis of simple models that oscillating axial (azimuthal) currents [72] or a steady axial (azimuthal) motion of the LIMPUS magnetic field configuration with respect to the plasma column [73] may suppress the described instabilities. The time scale of these processes is given, among other parameters, by the growth times of the instabilities of interest.

In applying stabilisation by oscillating axial currents, as planned in connection with the Scyllac project [17], the problem arises that an anomalous resistivity is required for the rapidly fluctuating magnetic field configuration to penetrate the region of rarefied plasma (in the density range from 10^{12} to 10^{14} cm[13]) surrounding the high β plasma column to be stabilised. Experiments by VAN DER LAAN, VAN DONSELAAR and MEWE [74] in an alternating screw pinch have shown that in these low β external plasma regions a layer is formed enveloping the high β plasma column and conducting the axial current, which process in the absence of ano-

[72] E. S. WEIBEL, Phys. Fluids **3**, 946 [1960].
[73] F. HAAS and J. WESSON, Phys. Rev. Lett. **19**, 833 [1967].
[74] P. C. T. VAN DER LAAN, M. F. VAN DONSELAAR, and R. MEWE, First European Conf. CFPP, München 1966.

malous resistivity might affect the intended dynamic stabilisation. However, the authors of the Scyllac proposal [17] have proved their expectation [75] that in the case of high current densities two-stream instabilities can (e. g. [76]) occur in those layers as a mechanism to reduce classical conductivity.

With the stabilization by means of a LIMPUS magnetic field configuration moving as a travelling wave relative to the plasma column (phase velocity of the wave larger than propagation velocity of the perturbation) the problem arises that under realistic conditions an acceleration of the plasma in the direction of wave propagation must be expected. In the Culham 8 m Theta Pinch [66], provision is therefore made for the LIMPUS configuration to be impressed on the plasma as a standing wave [77, 78]. Since with the last method only oscillating currents perpendicularly to the confining magnetic field are involved, the problem of low density boundary regions appears less critical.

The static M & S configuration belongs to a group of toroidal configurations in which single particles are temporarily trapped on drift surfaces in regions of low field strength, and may thus contribute to enhanced diffusion. In the planned standing-wave stabilisation experiments, the field oscillations will be of the order of the ion transit time over a period length. For this case the theory of trapped particle diffusion has not yet been treated.

Instead of attempting to stabilise the MHD-unstable M & S configuration by dynamic methods, it might seem simpler to look for MHD-stable static configurations appropriate to highly compressed high β plasmas [33, 56, 58, 79]. However, theory has not yet predicted configurations of this type which could be used for toroidal theta pinches in a simple way. Thus far all approaches which have been considered for the confinement of toroidal theta pinch plasmas in a stable static equilibrium configuration have appeared to involve problems comparable with M & S systems. Further M & S experiments directed towards methods of suppressing MHD instabilities can therefore contribute to an understanding in this field.

Acknowledgements

The author gratefully acknowledges the continuous and stimulating support of Prof. Dr. E. FÜNFER, Dr. G. v. GIERKE and in particular Prof. Dr. A. SCHLÜTER. He would especially like to thank his colleagues [81], who cooperated on the experiments described. They contributed to this report in addition by many valuable discussions and criticisms, for which the author would also like to thank Drs. G. GRIEGER, F. HAAS, P. MERKEL, D. PFIRSCH, W. QUINN, F. RIBE, H. U. SCHMIDT, J. WESSON and especially H. WOBIG. The author is further indebted to L. RONSON for the English translation and to Dr. W. ELLIS, whose assistance in preparing the present version was most valuable.

[75] E. M. LITTLE, A. A. NEWTON, W. E. QUINN, and F. L. RIBE, PPCNFR, CN-24/K-2 Novosibirsk 1968.

[76] A. SIMON, Plasma Physics, B. 163, IAEA Wien 1965.

[77] G. BERGE, PPCNFR CN-24/J-11, Novosibirsk 1968.

[78] Recent results have indeed shown that the MHD instability of a bulged theta pinch plasma could be suppressed for the duration of the oscillating field [80].

[79] B. B. KADOMTSEV, Plasma Physics and the Problem of Controlled Thermonuclear Reactions, IV, 27, Pergamon Press, London 1960.

[80] H. A. B. BODIN, E. P. BUTT, J. MCCARTAN, and G. H. WOLF, Dynamic Stabilisation of an $m=1$ Instability, 3rd Europ. Conf. Plasma Phys. and Contr. Fusion, Utrecht 1969.

[81] Munich M & S Experiments: E. REMY, U. GROSSMANN-DOERTH, J. JUNKER, W. LOTZ, and F. RAU. — Munich LIMPUS Experiment: C. ANDELFINGER, G. DECKER, E. FÜNFER, E. REMY, M. ULRICH, and H. WOBIG. — Culham Stability Experiment: H. A. B. BODIN, A. A. NEWTON, and J. WESSON.